We have a good chance to make the centennial

Rainer Weiss, MIT on behalf of the
VIRGO/LIGO Scientific Collaboration

GW2010
University of Minnesota
Twin Cities
Oct 15, 2010

What centennial?

“*Subtle is the Lord*” A scientific biography of Einstein
Abraham Pais

“Raffiniert is der Herrgott aber böshaft ist Er nicht”

“*Einstein*”
Walter Isaacson

Personal recollection
Henry Stroke

SITZUNGSBERICHTE 1916.
XXXIII.
DER
KÖNIGLICH PREUSSISCHEN
AKADEMIE DER WISSENSCHAFTEN.

Näherungsweise Integration der Feldgleichungen der Gravitation.

Von A. Einstein.

$$\gamma'_{\mu\nu} = \alpha_{\mu\nu} f(x_1 + i x_4) = \alpha_{\mu\nu} f(x - t) . \tag{15}$$

Dabei sind die $\alpha_{\mu\nu}$ Konstante; f ist eine Funktion des Arguments $x - t$. Ist der betrachtete Raum frei von Materie, d. h. verschwinden die $T_{\mu\nu}$, so sind die Gleichungen (6) durch diesen Ansatz erfüllt. Die Gleichungen (4) liefern zwischen den $\alpha_{\mu\nu}$ die Beziehungen

$$\left.\begin{aligned} \alpha_{11} + i\alpha_{14} &= 0 \\ \alpha_{12} + i\alpha_{24} &= 0 \\ \alpha_{13} + i\alpha_{34} &= 0 \\ \alpha_{14} + i\alpha_{44} &= 0 \end{aligned}\right\} . \tag{16}$$

Von den 10 Konstanten $\alpha_{\mu\nu}$ sind daher nur 6 frei wählbar. Wir können die allgemeinste Welle der betrachteten Art daher aus Wellen von folgenden 6 Typen superponieren

$$\left.\begin{array}{llllll} \text{a)} & \begin{array}{l} \alpha_{11} + i\alpha_{14} = 0 \\ \alpha_{14} + i\alpha_{44} = 0 \end{array} & \begin{array}{l} \text{b)} \\ \text{c)} \end{array} & \begin{array}{l} \alpha_{12} + i\alpha_{24} = 0 \\ \alpha_{13} + i\alpha_{34} = 0 \end{array} & \begin{array}{l} \text{d)} \\ \text{e)} \\ \text{f)} \end{array} & \begin{array}{l} \alpha_{22} \neq 0 \\ \alpha_{23} \neq 0 \\ \alpha_{33} \neq 0 \end{array} \end{array}\right\} . \tag{17}$$

$$\begin{aligned} \text{d)}\quad \frac{1}{i}\, t_{22} &= \frac{f'^2}{4\varkappa}\, \alpha_{22}^2 = \frac{1}{4\varkappa}\left(\frac{\partial \gamma'_{22}}{\partial t}\right)^2 \\ \text{e)}\quad \frac{1}{i}\, t_{23} &= \frac{f'^2}{4\varkappa}\, \alpha_{23}^2 = \frac{1}{4\varkappa}\left(\frac{\partial \gamma'_{23}}{\partial t}\right)^2 \\ \text{f)}\quad \frac{1}{i}\, t_{33} &= \frac{f'^2}{4\varkappa}\, \alpha_{33}^2 = \frac{1}{4\varkappa}\left(\frac{\partial \gamma'_{33}}{\partial t}\right)^2 . \end{aligned}$$

Es ergibt sich also, daß nur die Wellen des letzten Typs Energie transportieren, und zwar ist der Energietransport einer beliebigen ebenen Welle gegeben durch

$$I_x = \frac{1}{i}\, t_{41} = \frac{1}{4\varkappa}\left[\left(\frac{\partial \gamma'_{22}}{\partial t}\right)^2 + 2\left(\frac{\partial \gamma'_{23}}{\partial t}\right)^2 + \left(\frac{\partial \gamma'_{33}}{\partial t}\right)^2\right] . \tag{18}$$

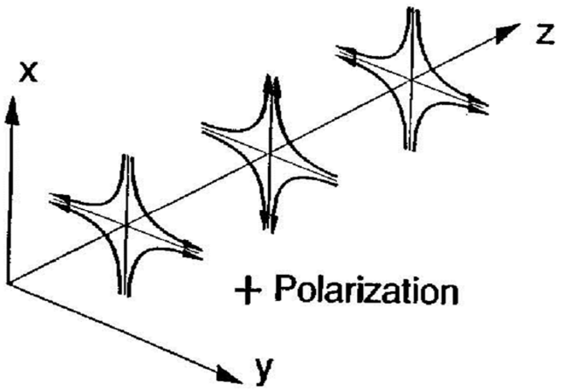
x
z
y
+ Polarization

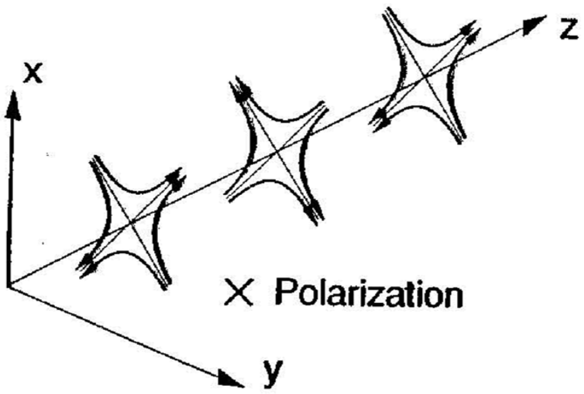
x
z
y
× Polarization

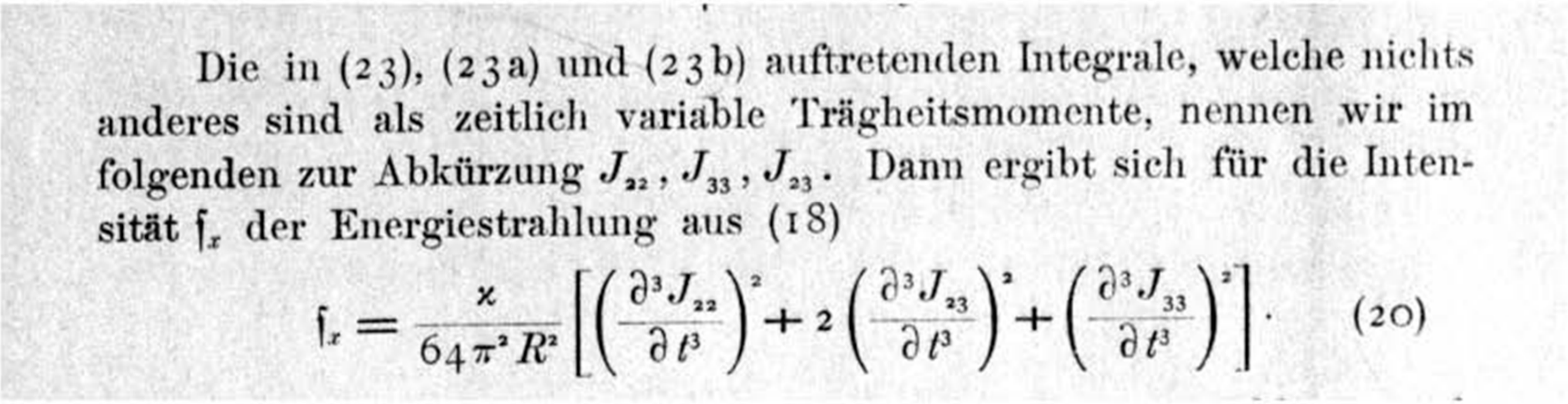

Die in (23), (23a) und (23b) auftretenden Integrale, welche nichts anderes sind als zeitlich variable Trägheitsmomente, nennen wir im folgenden zur Abkürzung J_{22}, J_{33}, J_{23}. Dann ergibt sich für die Intensität $\mathfrak{f}_x$ der Energiestrahlung aus (18)

$$\mathfrak{f}_x = \frac{\varkappa}{64\pi^2 R^2}\left[\left(\frac{\partial^3 J_{22}}{\partial t^3}\right)^2 + 2\left(\frac{\partial^3 J_{23}}{\partial t^3}\right)^2 + \left(\frac{\partial^3 J_{33}}{\partial t^3}\right)^2\right]. \qquad (20)$$

SPHERICALLY SYMMETRIC MOTION RADIATES GRAVITATIONAL WAVES

1918 VI. VII. VIII

SITZUNGSBERICHTE

DER

KÖNIGLICH PREUSSISCHEN

AKADEMIE DER WISSENSCHAFTEN

BERLIN 1918
VERLAG DER KÖNIGLICHEN AKADEMIE DER WISSENSCHAFTEN
IN KOMMISSION BEI GEORG REIMER

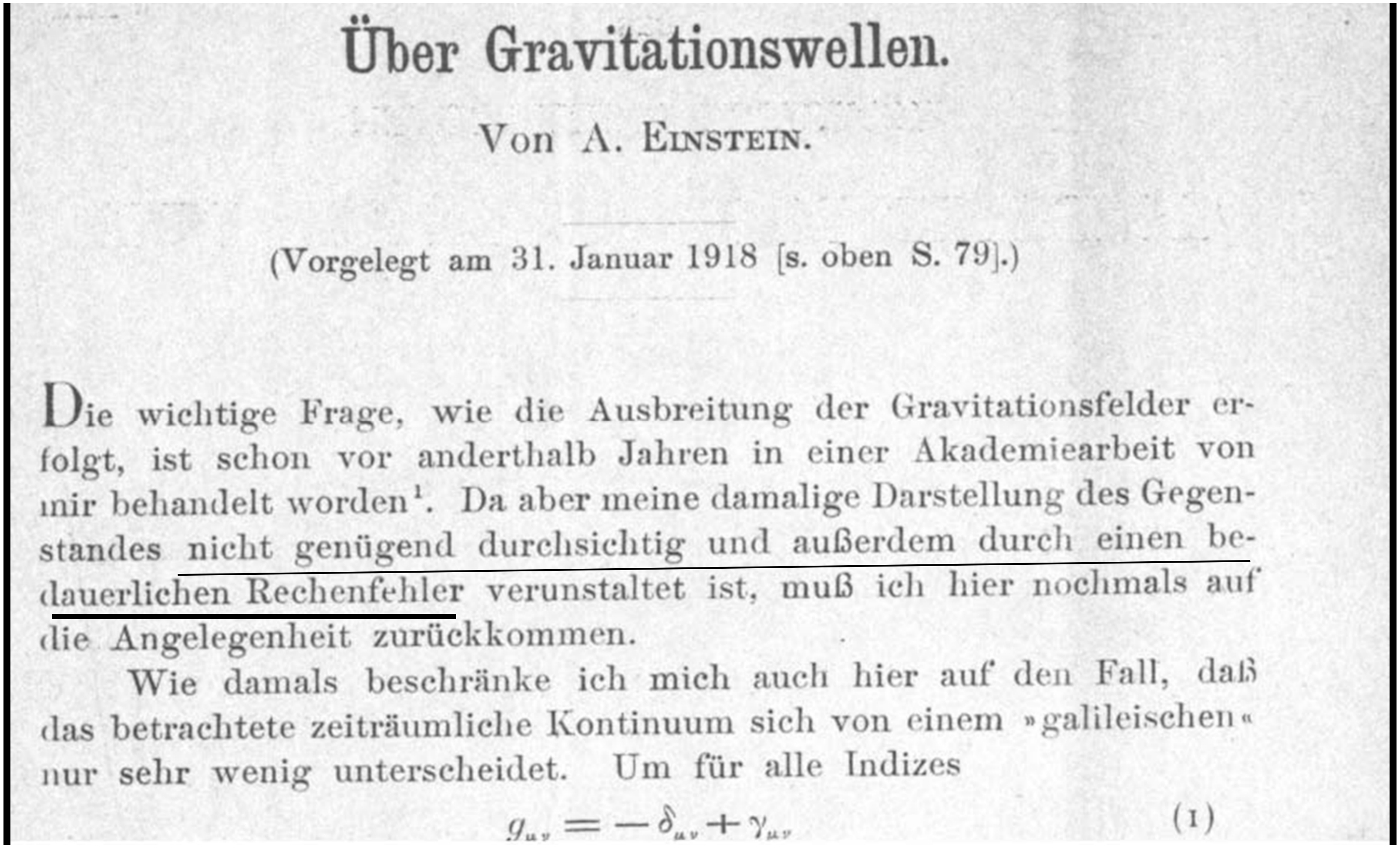

Über Gravitationswellen.

Von A. Einstein.

(Vorgelegt am 31. Januar 1918 [s. oben S. 79].)

Die wichtige Frage, wie die Ausbreitung der Gravitationsfelder erfolgt, ist schon vor anderthalb Jahren in einer Akademiearbeit von mir behandelt worden[1]. Da aber meine damalige Darstellung des Gegenstandes nicht genügend durchsichtig und außerdem durch einen bedauerlichen Rechenfehler verunstaltet ist, muß ich hier nochmals auf die Angelegenheit zurückkommen.

Wie damals beschränke ich mich auch hier auf den Fall, daß das betrachtete zeiträumliche Kontinuum sich von einem »galileischen« nur sehr wenig unterscheidet. Um für alle Indizes

$$g_{\mu\nu} = -\delta_{\mu\nu} + \gamma_{\mu\nu} \qquad (1)$$

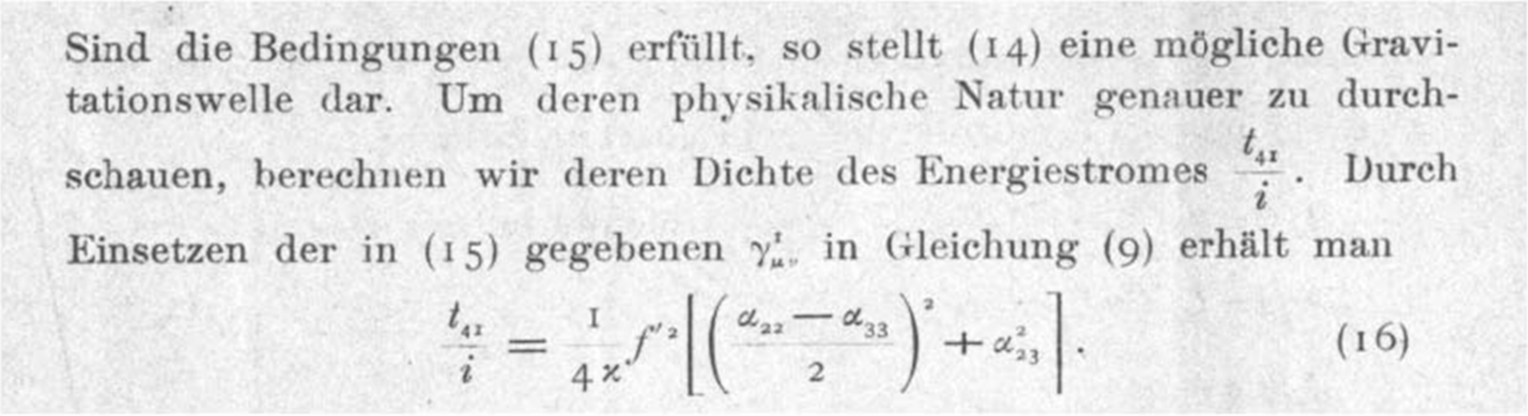

Sind die Bedingungen (15) erfüllt, so stellt (14) eine mögliche Gravitationswelle dar. Um deren physikalische Natur genauer zu durchschauen, berechnen wir deren Dichte des Energiestromes $\frac{t_{41}}{i}$. Durch Einsetzen der in (15) gegebenen $\gamma'_{\mu\nu}$ in Gleichung (9) erhält man

$$\frac{t_{41}}{i} = \frac{1}{4\varkappa} f'^2 \left[\left(\frac{\alpha_{22} - \alpha_{33}}{2} \right)^2 + \alpha_{23}^2 \right]. \qquad (16)$$

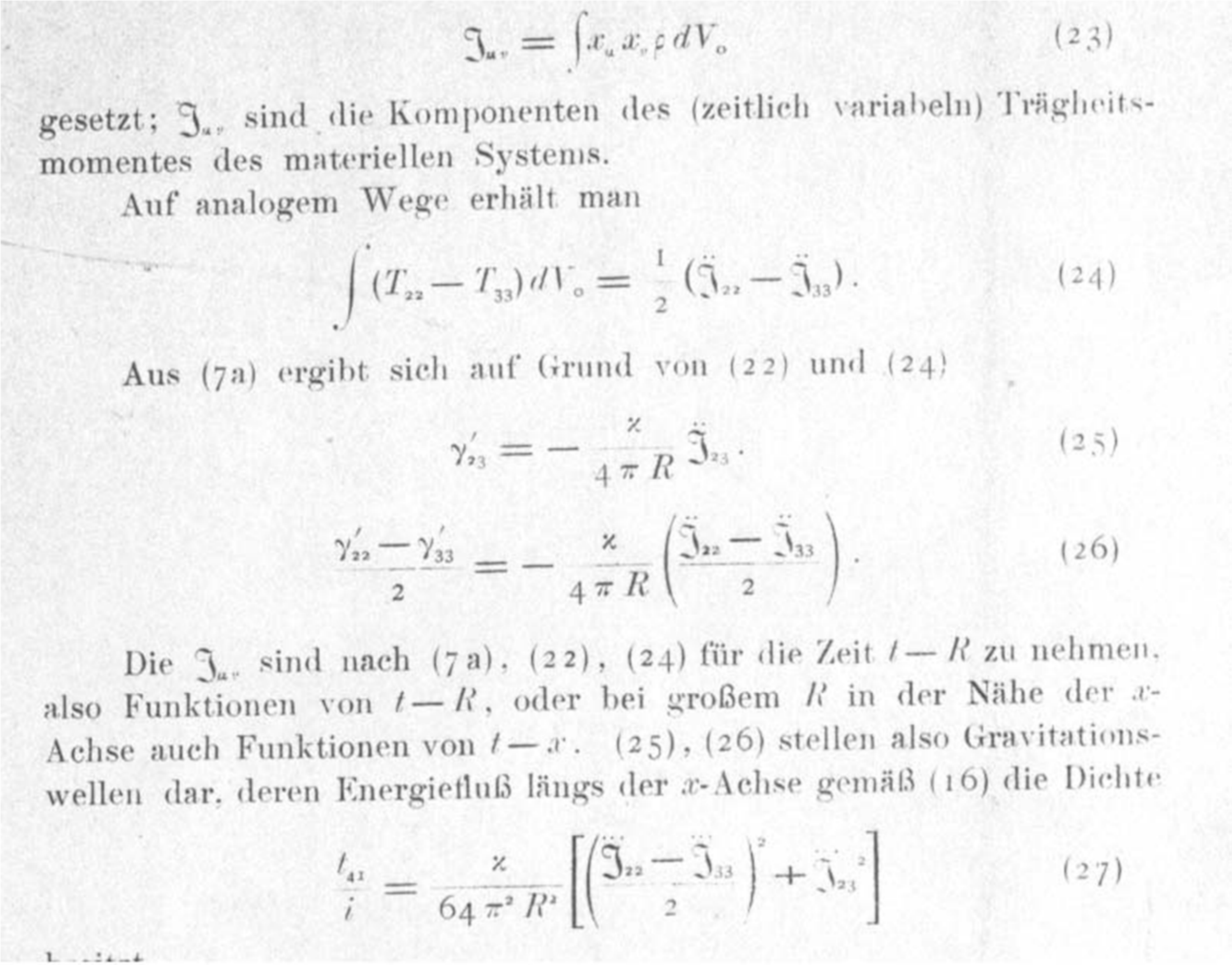

$$\mathfrak{J}_{\mu\nu} = \int x_\mu x_\nu \rho \, dV_0 \qquad (23)$$

gesetzt; $\mathfrak{J}_{\mu\nu}$ sind die Komponenten des (zeitlich variabeln) Trägheitsmomentes des materiellen Systems.

Auf analogem Wege erhält man

$$\int (T_{22} - T_{33})\, dV_0 = \frac{1}{2}\left(\ddot{\mathfrak{J}}_{22} - \ddot{\mathfrak{J}}_{33}\right). \qquad (24)$$

Aus (7a) ergibt sich auf Grund von (22) und (24)

$$\gamma'_{23} = -\frac{\varkappa}{4\pi R}\,\ddot{\mathfrak{J}}_{23}. \qquad (25)$$

$$\frac{\gamma'_{22} - \gamma'_{33}}{2} = -\frac{\varkappa}{4\pi R}\left(\frac{\ddot{\mathfrak{J}}_{22} - \ddot{\mathfrak{J}}_{33}}{2}\right). \qquad (26)$$

Die $\mathfrak{J}_{\mu\nu}$ sind nach (7a), (22), (24) für die Zeit $t - R$ zu nehmen, also Funktionen von $t - R$, oder bei großem R in der Nähe der x-Achse auch Funktionen von $t - x$. (25), (26) stellen also Gravitationswellen dar, deren Energiefluß längs der x-Achse gemäß (16) die Dichte

$$\frac{t_{41}}{i} = \frac{\varkappa}{64\pi^2 R^2}\left[\left(\frac{\dddot{\mathfrak{J}}_{22} - \dddot{\mathfrak{J}}_{33}}{2}\right)^2 + \dddot{\mathfrak{J}}_{23}^{\,2}\right] \qquad (27)$$

THE QUADRUPOLE FORMULA A FACTOR OF 2 TOO SMALL

~100 years since 1916

- B modes in the Cosmic Background
  - periods of 10^{10} years
- Timing with millisecond pulsars
  - periods of ~ year
- LISA
  - periods of hours to minutes
- Ground based interferometers
  - periods of 100 to 0.1 milliseconds

LIGO Scientific Collaboration

- Australian Consortium for Interferometric Gravitational Astronom
- The Univ. of Adelaide
- Andrews University
- The Australian National Univ.
- The University of Birmingham
- California Inst. of Technology
- Cardiff University
- Carleton College
- Charles Sturt Univ.
- Columbia University
- Embry Riddle Aeronautical Univ.
- Eötvös Loránd University
- University of Florida
- German/British Collaboration for the Detection of Gravitational Waves
- University of Glasgow
- Goddard Space Flight Center
- Leibniz Universität Hannover
- Hobart & William Smith Colleges
- Inst. of Applied Physics of the Russian Academy of Sciences
- Polish Academy of Sciences
- India Inter-University Centre for Astronomy and Astrophysics
- Louisiana State University
- Louisiana Tech University
- Loyola University New Orleans
- University of Maryland
- Max Planck Institute for Gravitational Physics

- University of Michigan
- University of Minnesota
- The University of Mississippi
- Massachusetts Inst. of Technology
- Monash University
- Montana State University
- Moscow State University
- National Astronomical Observatory of Japan
- Northwestern University
- University of Oregon
- Pennsylvania State University
- Rochester Inst. of Technology
- Rutherford Appleton Lab
- University of Rochester
- San Jose State University
- Univ. of Sannio at Benevento, and Univ. of Salerno
- University of Sheffield
- University of Southampton
- Southeastern Louisiana Univ.
- Southern Univ. and A&M College
- Stanford University
- University of Strathclyde
- Syracuse University
- Univ. of Texas at Austin
- Univ. of Texas at Brownsville
- Trinity University
- Universitat de les Illes Balears
- Univ. of Massachusetts Amherst
- University of Western Australia
- Univ. of Wisconsin-Milwaukee
- Washington State University
- University of Washington

Mostly idealized and fundamental noise

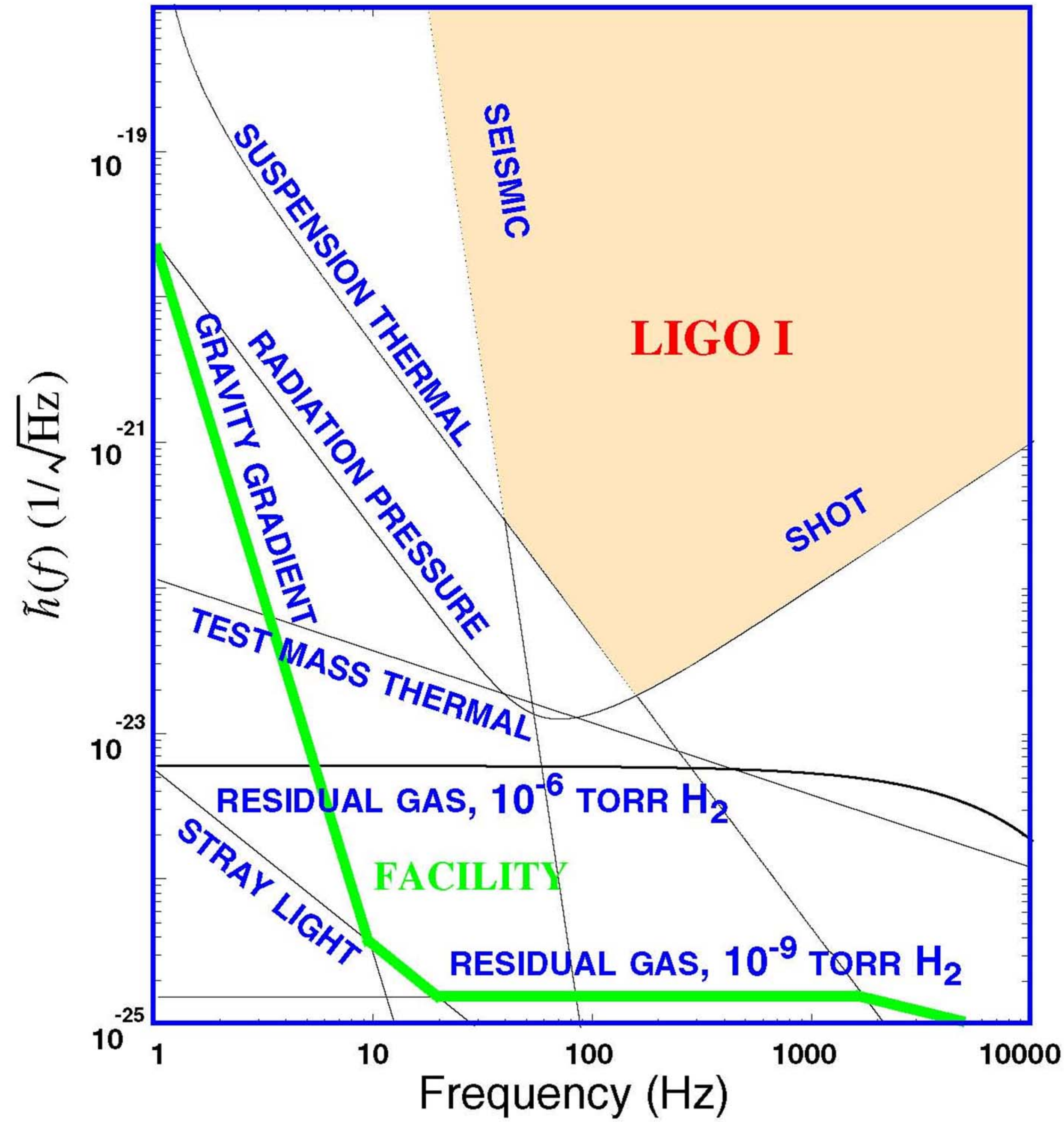

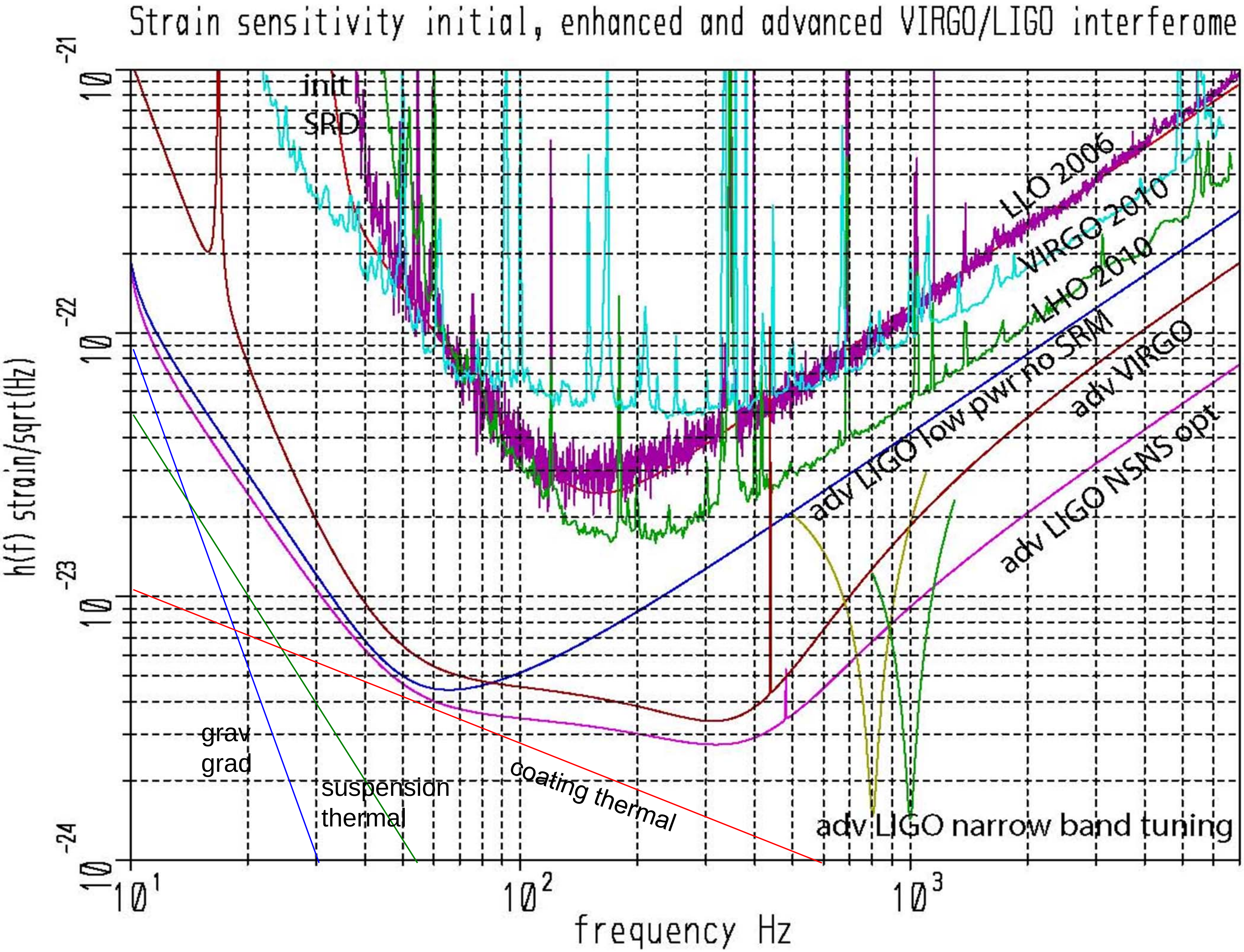
Strain sensitivity initial, enhanced and advanced VIRGO/LIGO interferome
init
SRD
LLO 2006
VIRGO 2010
LHO 2010
adv LIGO low pwr no SRM
adv VIRGO
adv LIGO NSNS opt
adv LIGO narrow band tuning
grav
grad
suspension
thermal
coating thermal
h(f) strain/sqrt(Hz)
10^{-21}
10^{-22}
10^{-23}
10^{-24}
10^{1}
10^{2}
10^{3}
frequency Hz

Program of detector improvements

- **Major steps between initial and advanced LIGO**
  - Increase laser input power 10 to 180 watts in stages
  - Incorporation of an output mode cleaner
  - Output optics and electro-optics chain in vacuum
  - DC (carrier offset) “modulation” technique
  - Reduction in thermal noise
    - Steel wire to fused silica fiber suspension elements
    - Lower mechanical dissipation optical coatings
    - Larger fused silica test masses : 10 kg to 40 kg
  - Improved active seismic isolation – extend sensitivity to 15Hz
  - Tunable dual recycling interferometer configuration
  - Quantum limited operation over significant band

BEGIN
IN
ENHANCED
LIGO

Seismic Isolation

Springs and Masses

damped spring
cross section

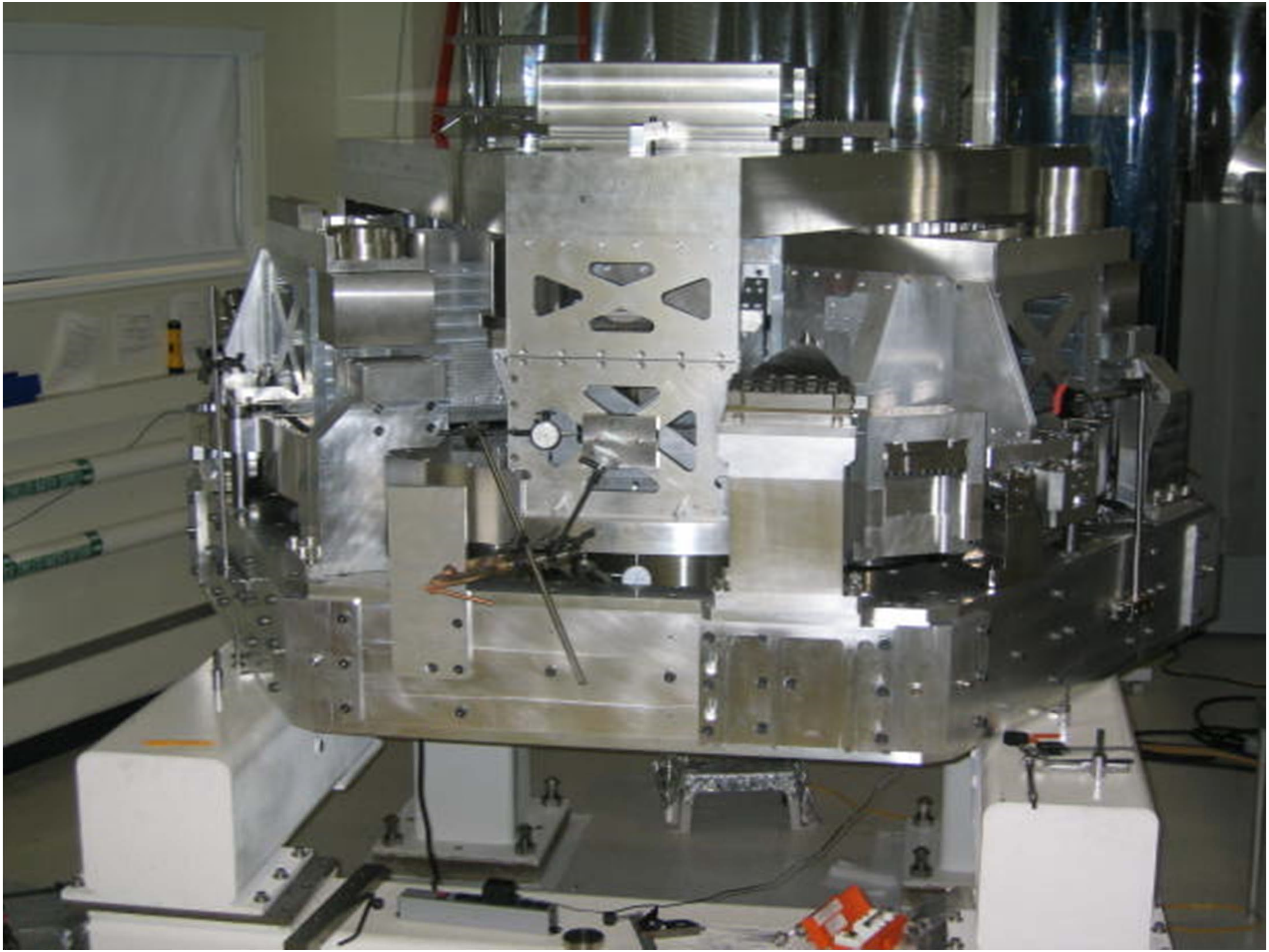

Seismic Isolation

suspension system

suspension assembly for a core optic

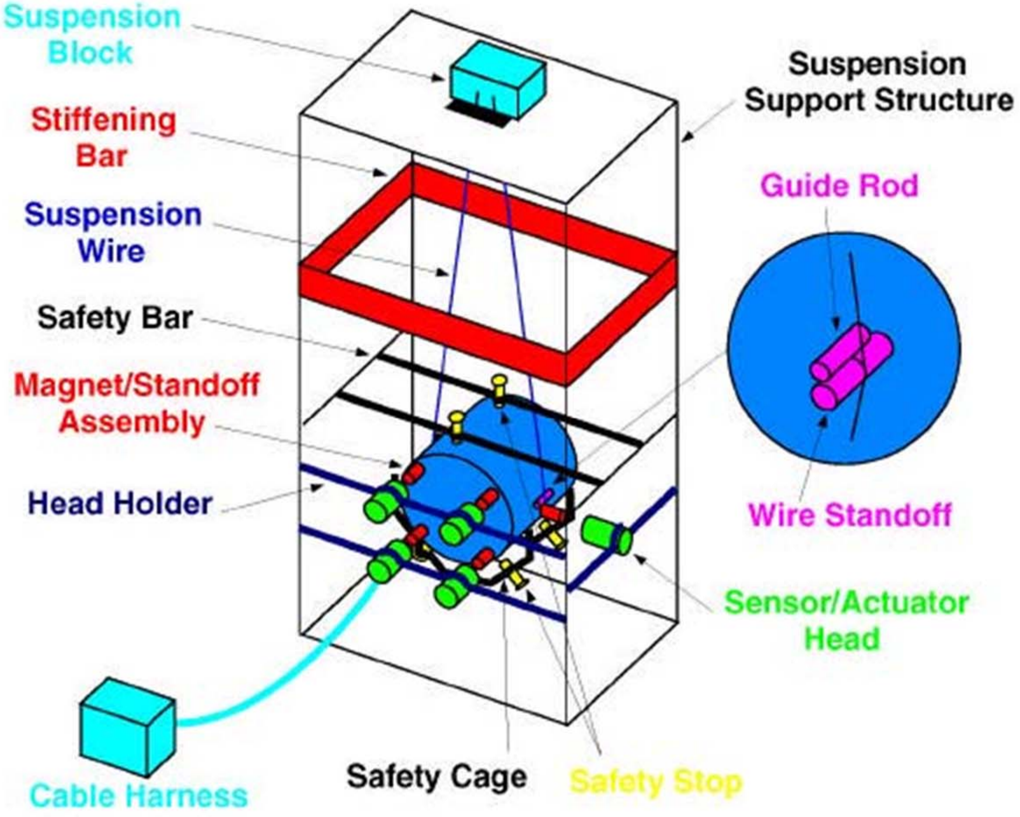

Core Optics

Suspension

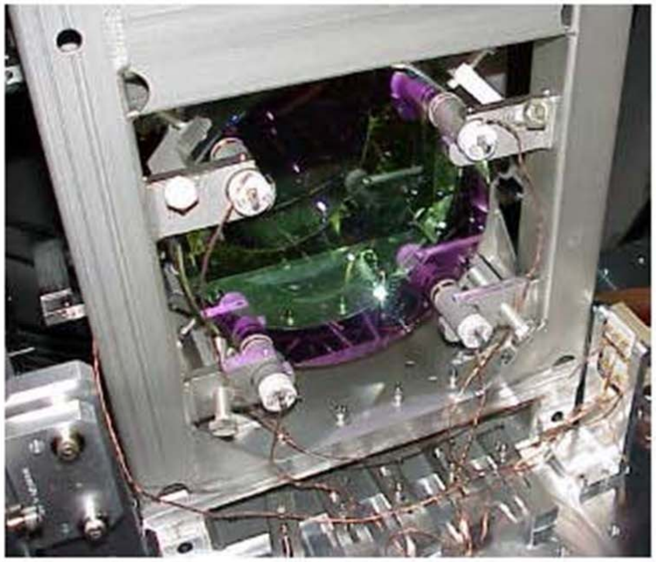

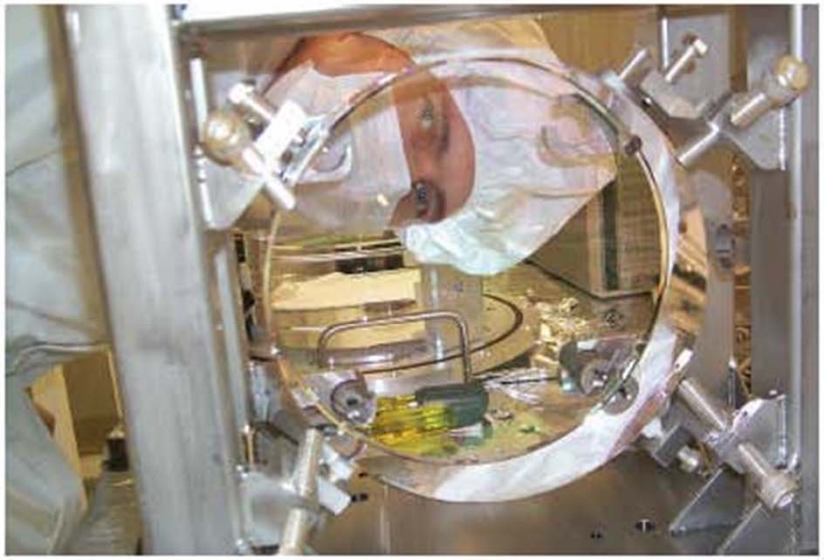

Schematic

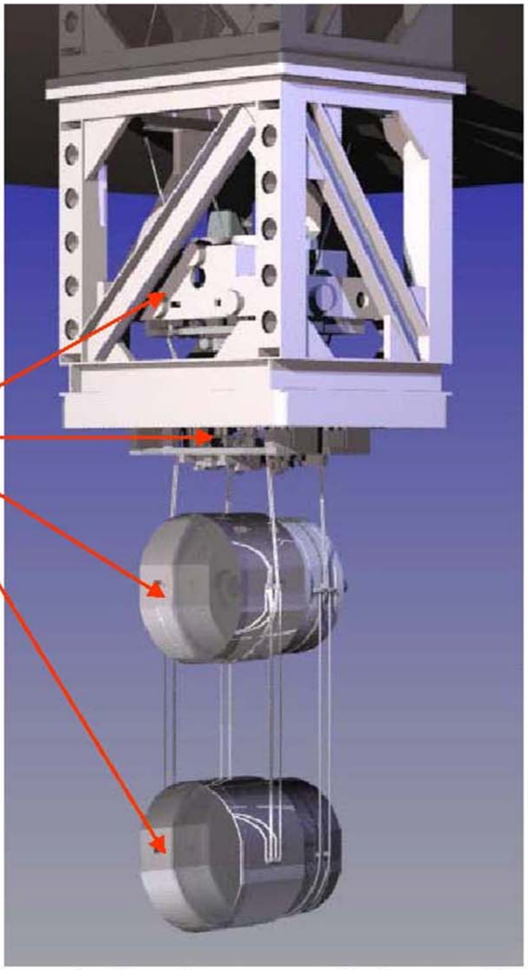

Four stages

Damping applied at top stage

LELAND STANFORD JUNIOR UNIVERSITY 1891

Main chain plus parallel reaction chain for control actuation

(Lower support structure removed for clarity)

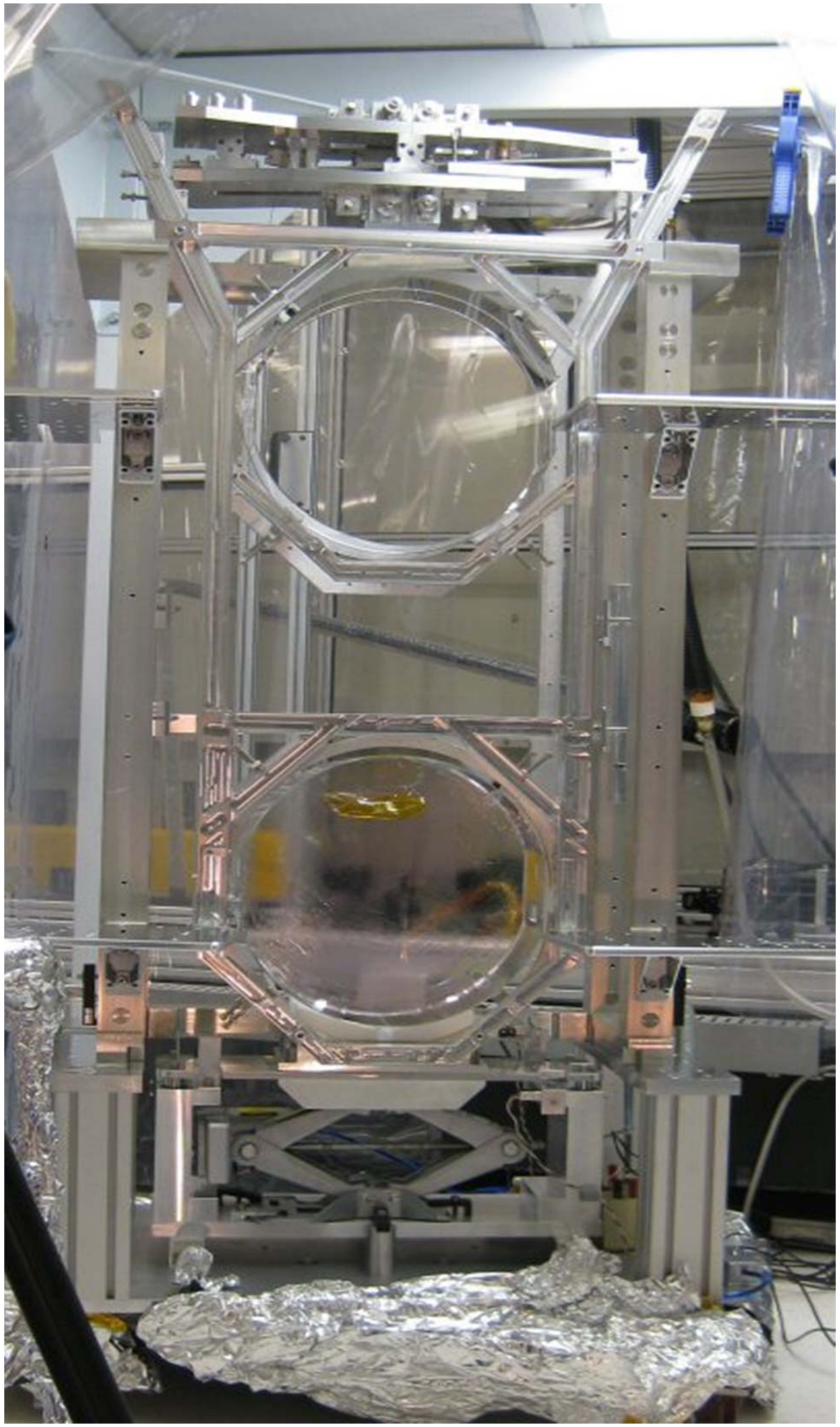

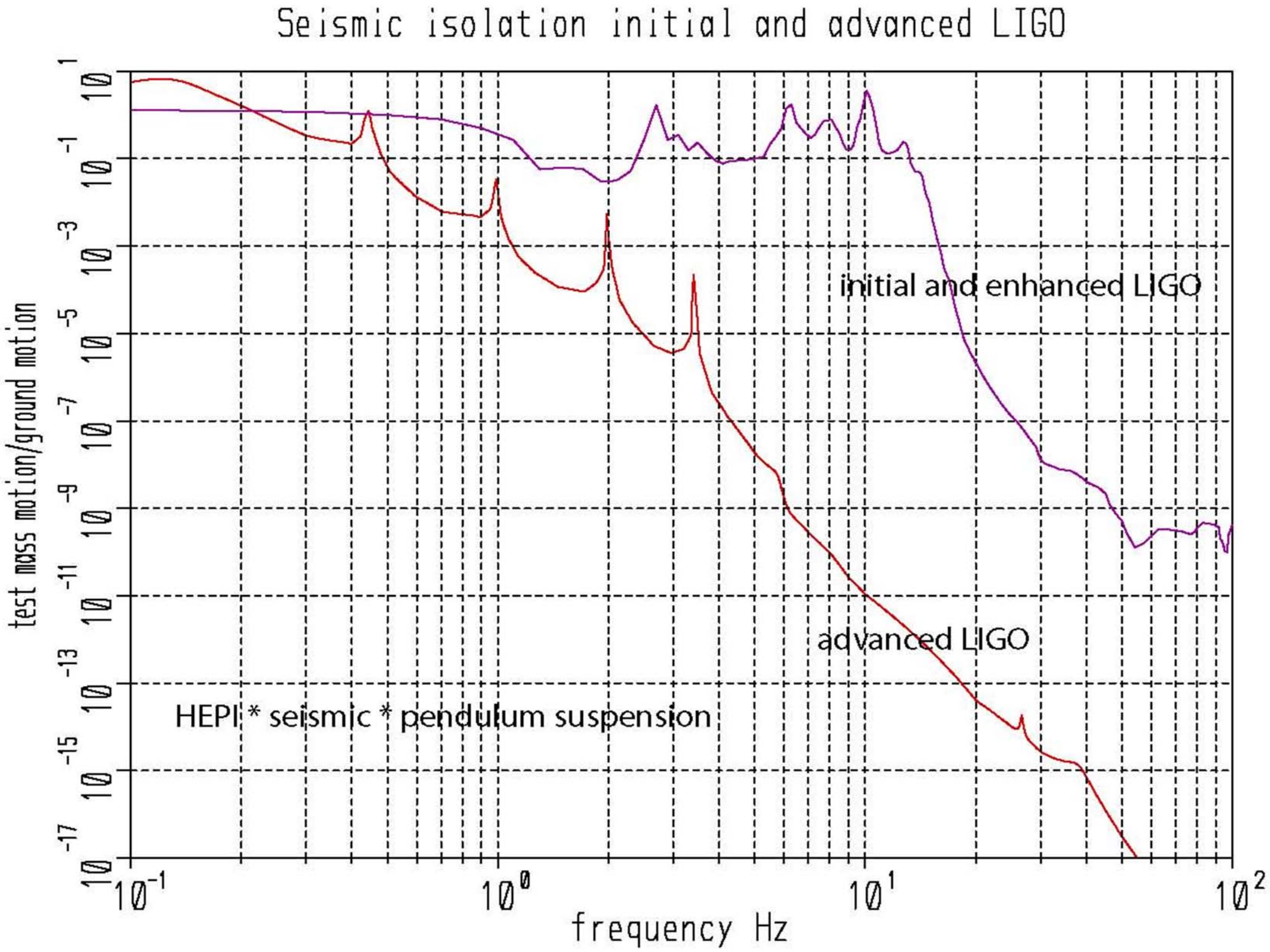
Seismic isolation initial and advanced LIGO
test mass motion/ground motion
10^{1}
10^{-1}
10^{-3}
10^{-5}
10^{-7}
10^{-9}
10^{-11}
10^{-13}
10^{-15}
10^{-17}
10^{-1}
10^{0}
10^{1}
10^{2}
frequency Hz
initial and enhanced LIGO
advanced LIGO
HEPI * seismic * pendulum suspension

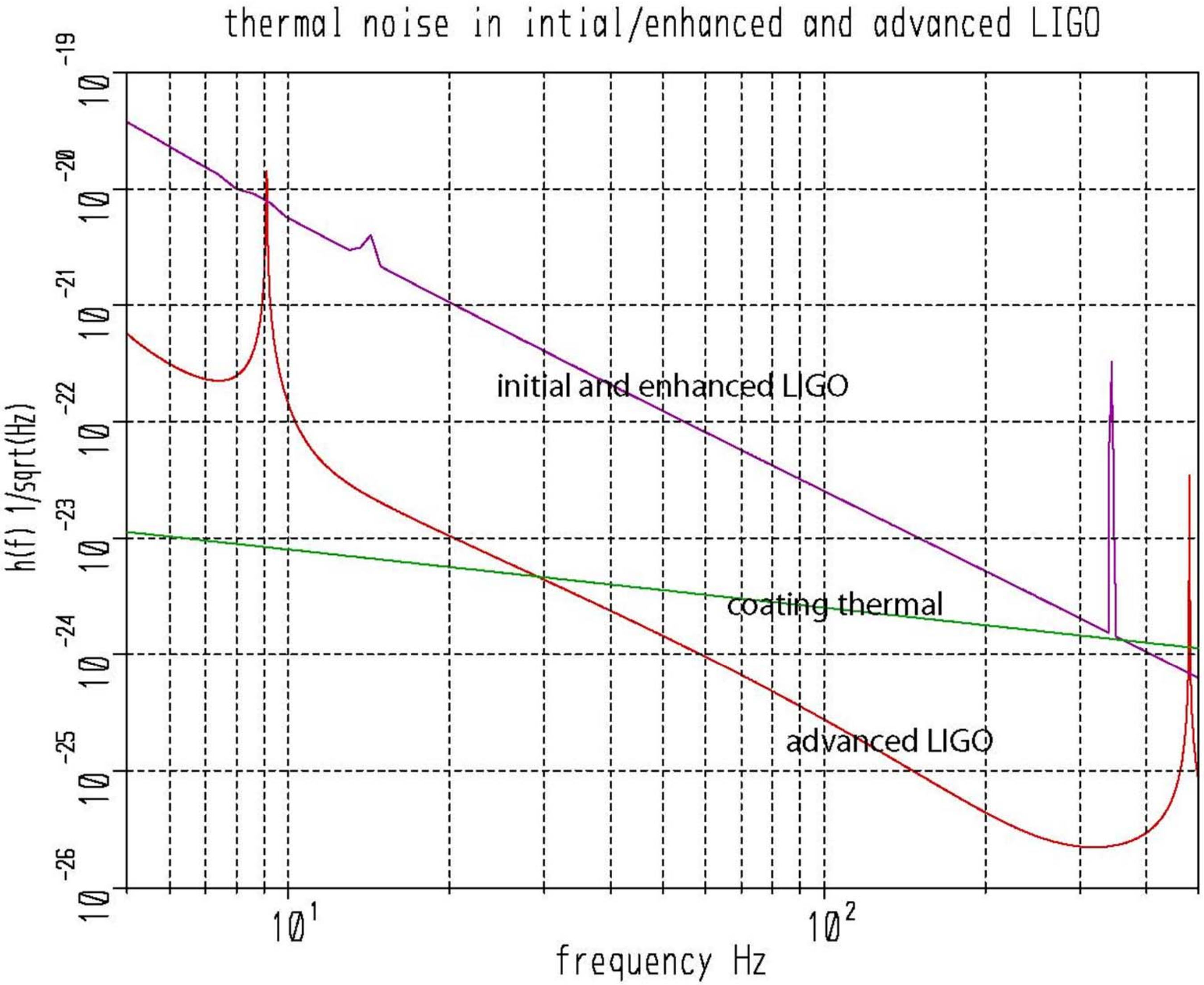
thermal noise in intial/enhanced and advanced LIGO
h(f) 1/sqrt(Hz)
10^-19
10^-20
10^-21
10^-22
10^-23
10^-24
10^-25
10^-26
10^1
10^2
frequency Hz
initial and enhanced LIGO
coating thermal
advanced LIGO

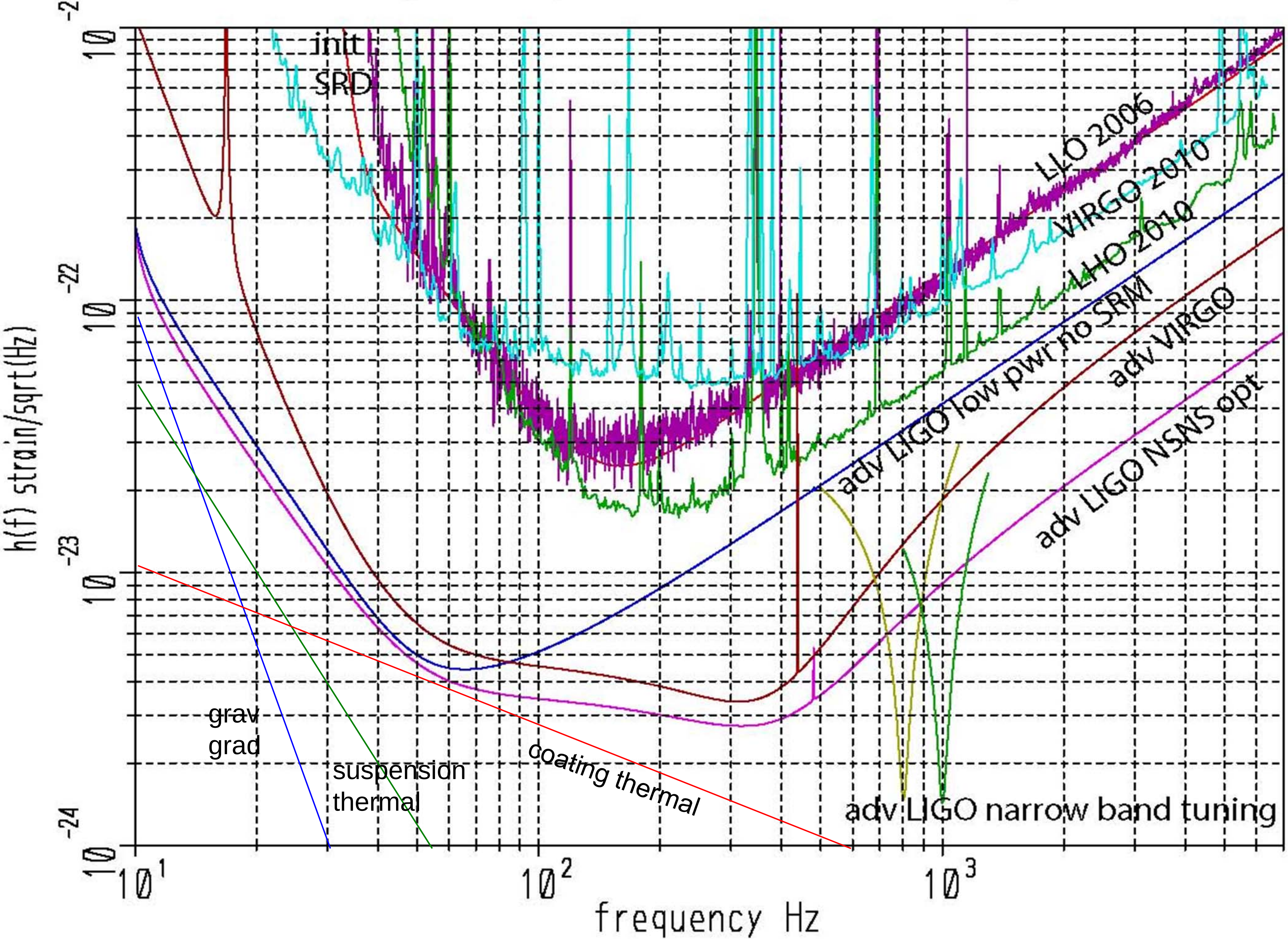

Strain sensitivity initial, enhanced and advanced VIRGO/LIGO interferome

Advanced LIGO broadband operational modes

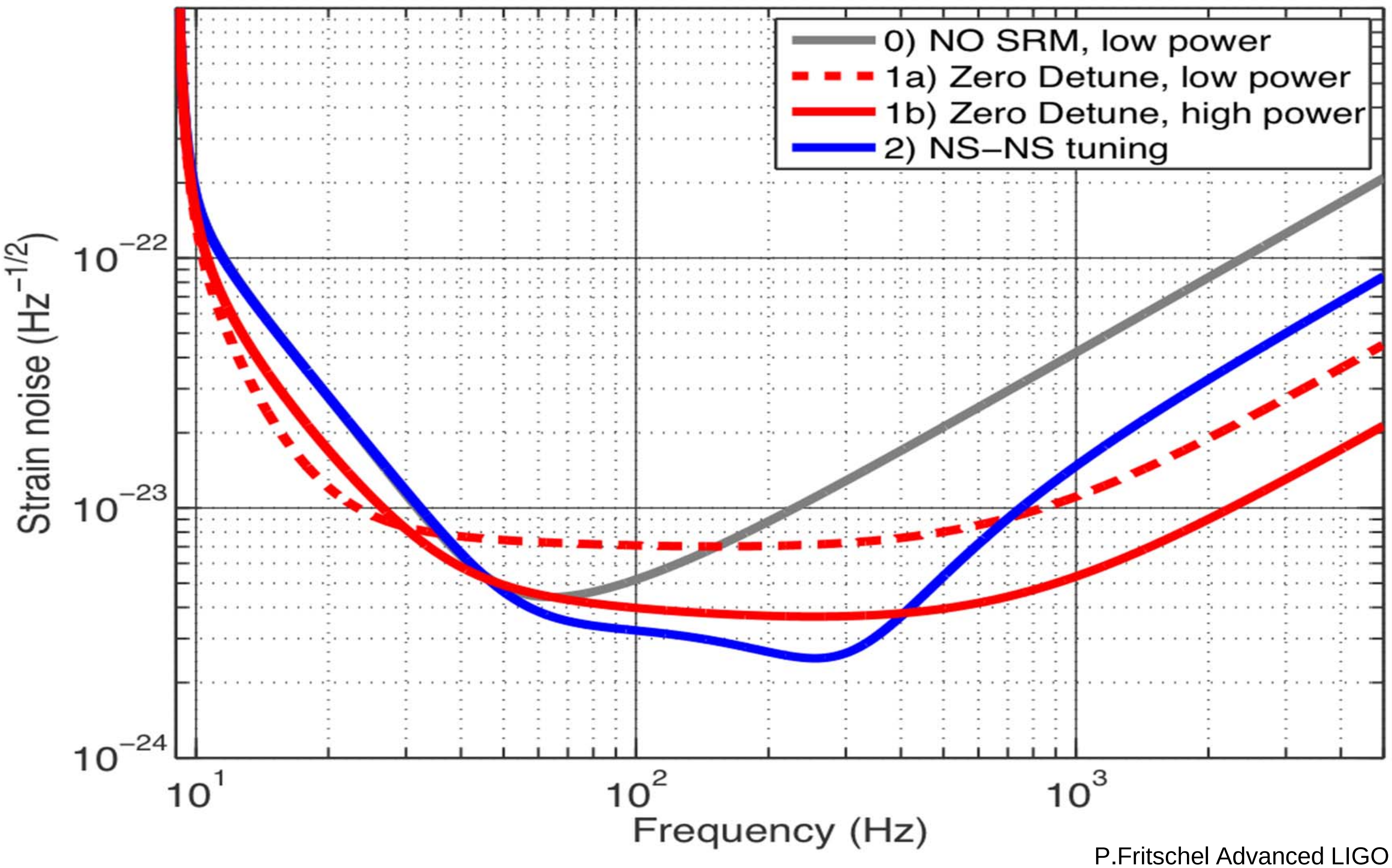

P.Fritschel Advanced LIGO Systems Design (2009)

Mode	*NS-NS Range*	*BH-BH Range*	P_{in}	T_{SRM}	ϕ_{SRC}	h_{RMS}, 10^{-22} (band)
0	150 Mpc	1.60 Gpc	25 W	100%	–	0.53 (40 – 140 Hz)
1a	145 Mpc	1.65 Gpc	25 W	20%	0 deg.	0.70 (110 – 210 Hz)
1b	190 Mpc	1.85 Gpc	125 W	20%	0 deg.	0.37 (205 – 305 Hz)
2	200 Mpc	1.65 Gpc	125 W	20%	16 deg.	0.25 (205 – 305 Hz)

R = horizon distance

Binary NS coalescences 1.4Mo / 1.4 Mo

Strain vs time

$$h(t) = \frac{2G}{Rc^4}\left(\frac{m_1 m_2}{m_1 + m_2}\right)(\pi G(m_1 + m_2)f(t))^{\frac{2}{3}} = 1.8\times10^{-23} f = 100\text{Hz} \;\; R = 100\text{Mpc}$$

$$f(t) = \frac{1}{\pi}\left(\frac{5}{256\tau}\right)^{\frac{3}{8}}\left(\frac{c^3}{G\,M_{chirp}}\right)^{\frac{5}{8}} = \frac{134\text{Hz}}{\tau^{\frac{3}{8}}} \qquad M_{chirp} = \frac{(m_1 m_2)^{\frac{3}{5}}}{(m_1 + m_2)^{\frac{1}{5}}} \qquad \tau = (t_{end} - t)$$

Frequency spectrum

$$h(f) = \frac{1}{\pi^{\frac{2}{3}}}\sqrt{\frac{5}{24}}\left(\frac{c}{R}\right)\left(\frac{G\,M_{chirp}}{c^3}\right)^{\frac{5}{6}}\left(\frac{1}{f^{\frac{7}{6}}}\right) = \frac{9.1\times10^{-22}}{f^{\frac{7}{6}}}\text{strain/Hz} \;\; R = 100\text{Mpc}$$

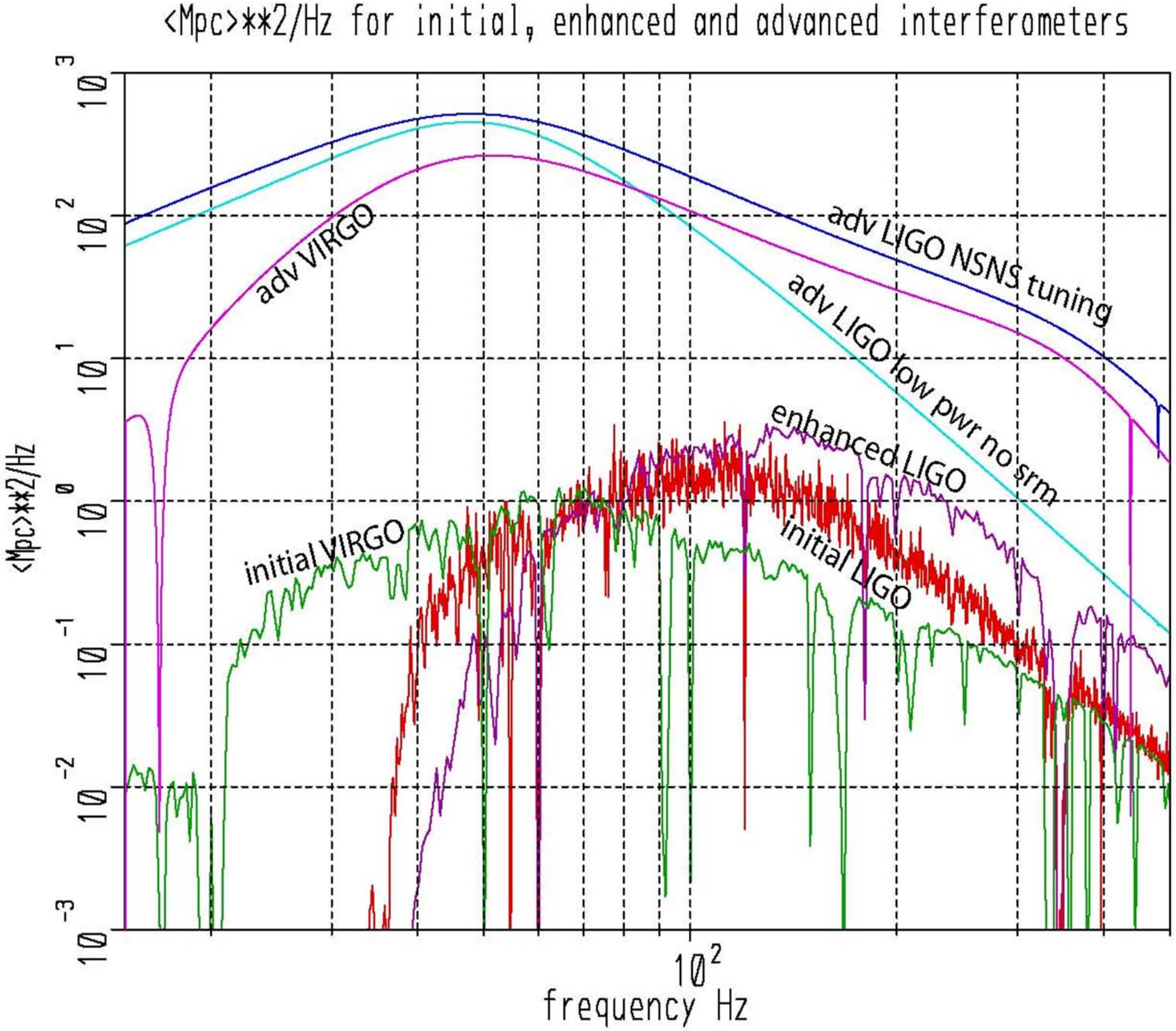

$$h_{\text{signal}}(f)=\sqrt{h_x^2(f)+h_+^2(f)}$$

$$\text{SNR}^2 = 2\int_0^\infty \frac{h_{\text{signal}}^2(f)}{h_{\text{noise}}^2(f)}\,df$$

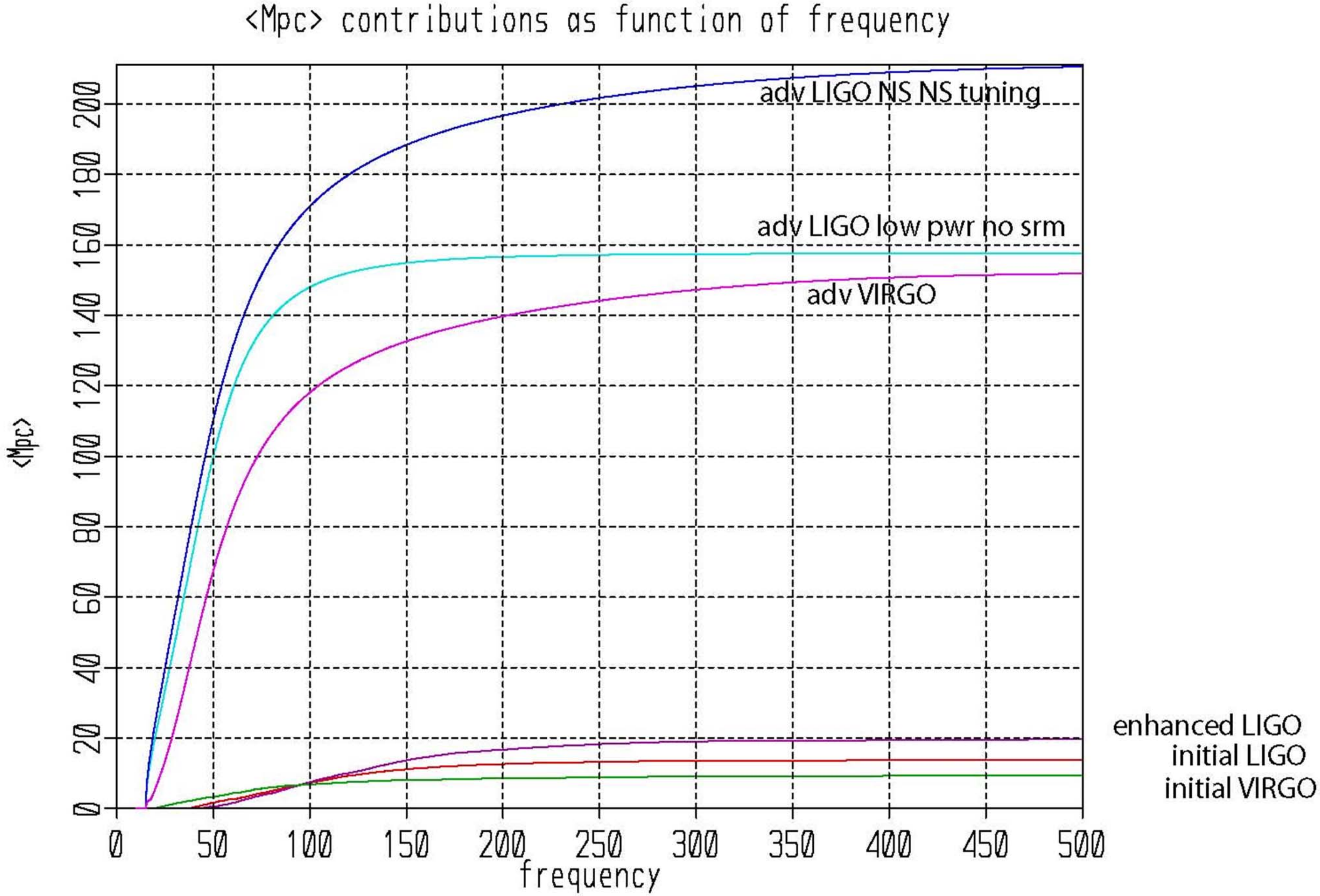

<Mpc> contributions as function of frequency
<Mpc>
0
20
40
60
80
100
120
140
160
180
200
0
50
100
150
200
250
300
350
400
450
500
frequency
adv LIGO NS NS tuning
adv LIGO low pwr no srm
adv VIRGO
enhanced LIGO
initial LIGO
initial VIRGO

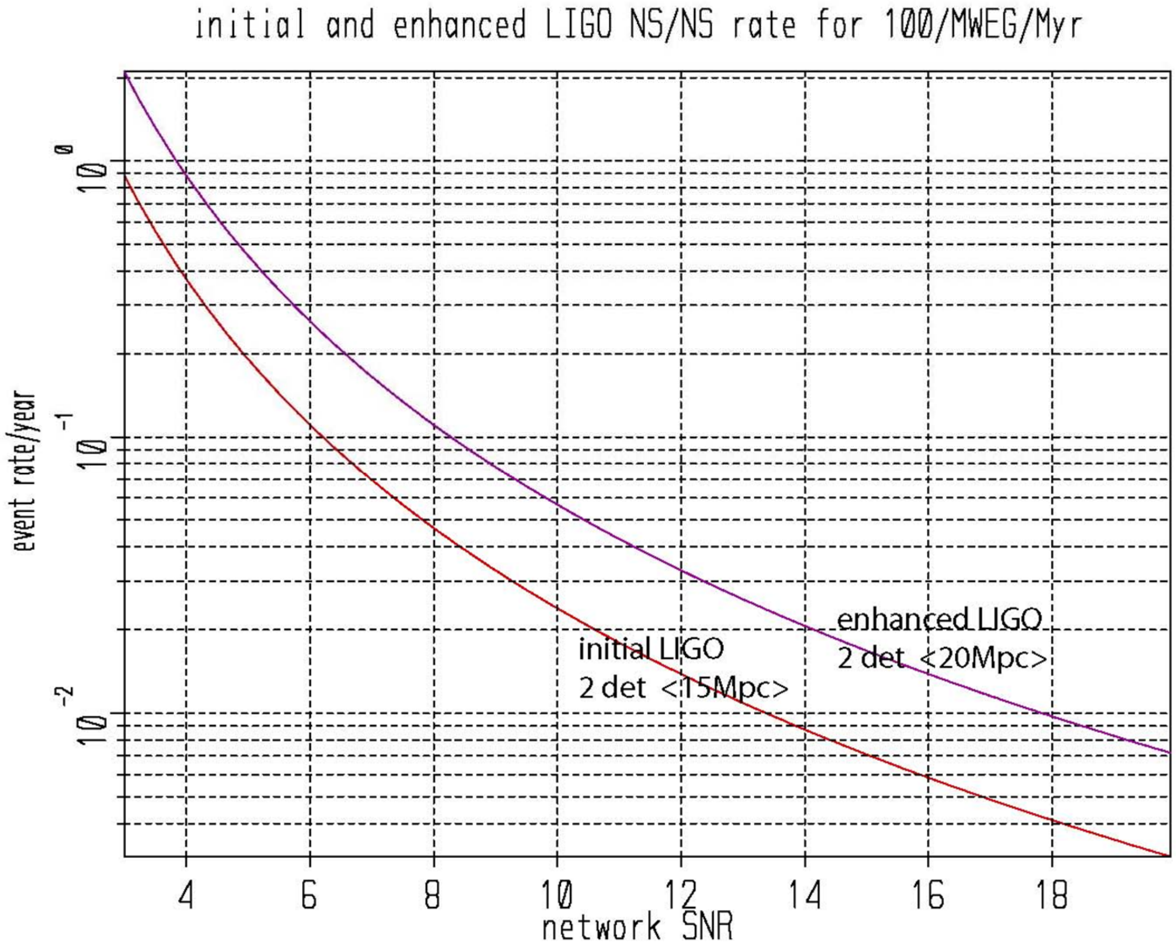

initial and enhanced LIGO NS/NS rate for 100/MWEG/Myr

Conditions:

False alarm rates reduced to Gaussian statistics.

Coherent detection

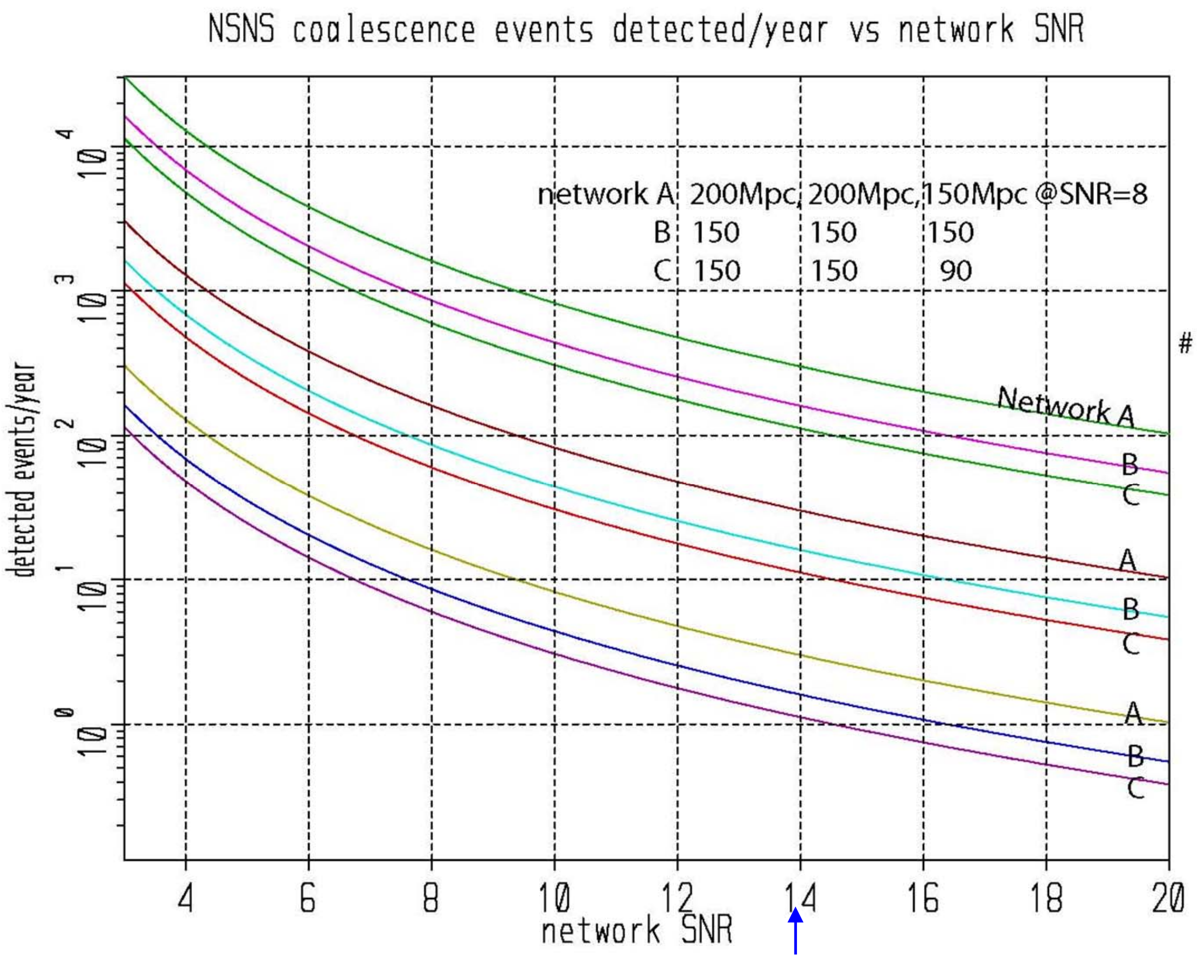

MWEG/Mpc^3 = 0.012

insp./MWEG/Myr

1000

100

10

SNR = 8/det

$$\text{NSNS events/year} = \frac{4\pi}{3}\left(\frac{8}{\text{SNR}_{\text{network}}}\sqrt{\sum_{1}^{\text{n det}}\left\langle R(\text{Mpc})\right\rangle^{2}_{\text{SNR}=8}}\right)^{3}\left(\frac{\text{MWEG}}{\text{Mpc}^{3}}\right)\left(\frac{\#\text{NSNS insp}}{\text{MWEG/yr}}\right)$$

Spare slides follow

Physical Environment Monitoring

- Seismic motion
  - xyz seismometer/building
- Motion of test mass chambers
  - xyz accelerometers/chamber
- Acoustic excitation
  - microphone/building
- Magnetic fields
  - xyz magnetometer/building
  - xyz high sensitivity coil/site
- Radio Frequency interference
  - multiband 30kHz -100MHz receiver/site
- Main AC power monitor
  - 3 phase monitor/building
- Muon shower detector
  - scintillator-PM tube/site

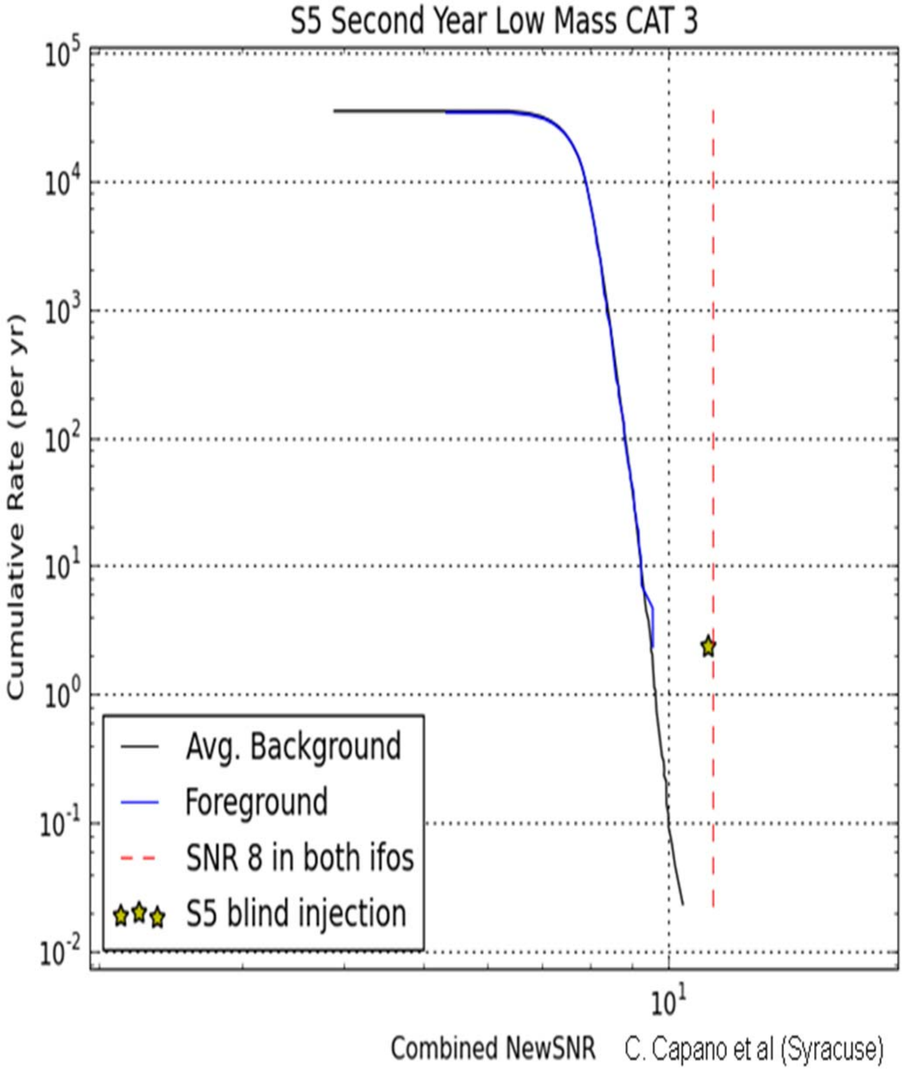

C. Capano et al (Syracuse)

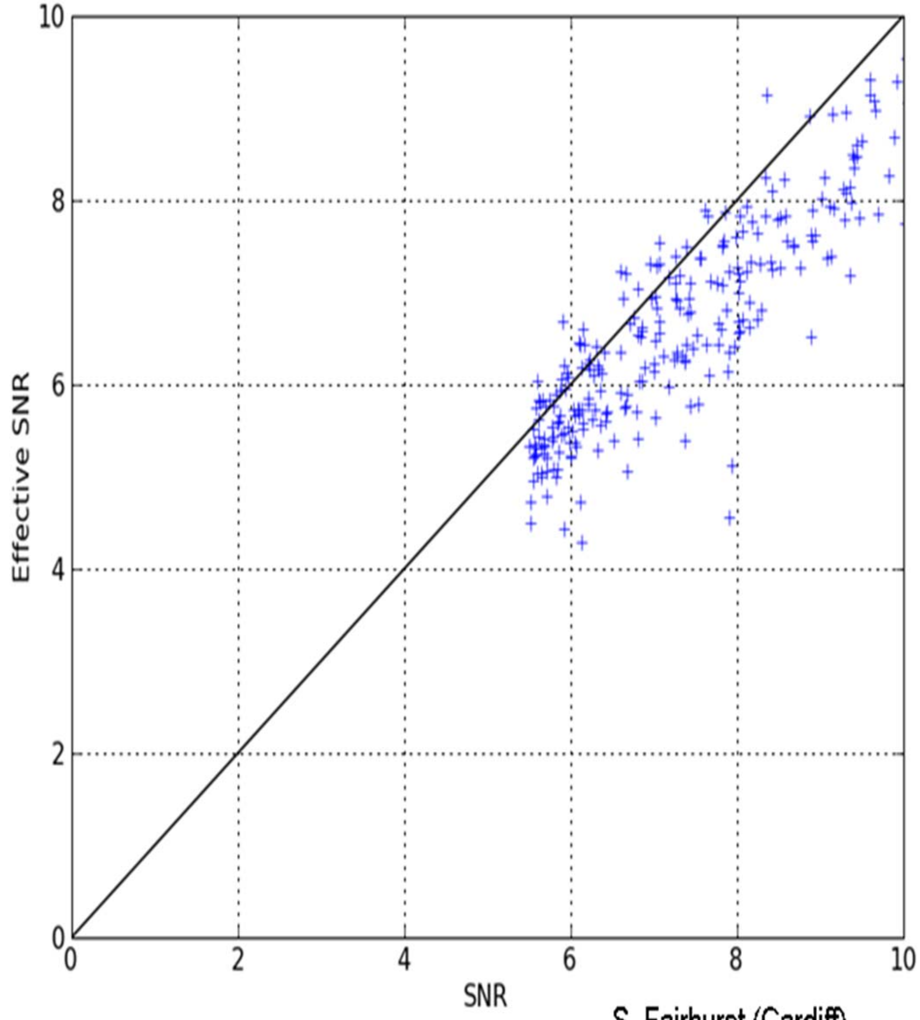

S. Fairhurst (Cardiff)

Spare slides follow

Physical Environment Monitoring

- Seismic motion
  - xyz seismometer/building
- Motion of test mass chambers
  - xyz accelerometers/chamber
- Acoustic excitation
  - microphone/building
- Magnetic fields
  - xyz magnetometer/building
  - xyz high sensitivity coil/site
- Radio Frequency interference
  - multiband 30kHz -100MHz receiver/site
- Main AC power monitor
  - 3 phase monitor/building
- Muon shower detector
  - scintillator-PM tube/site

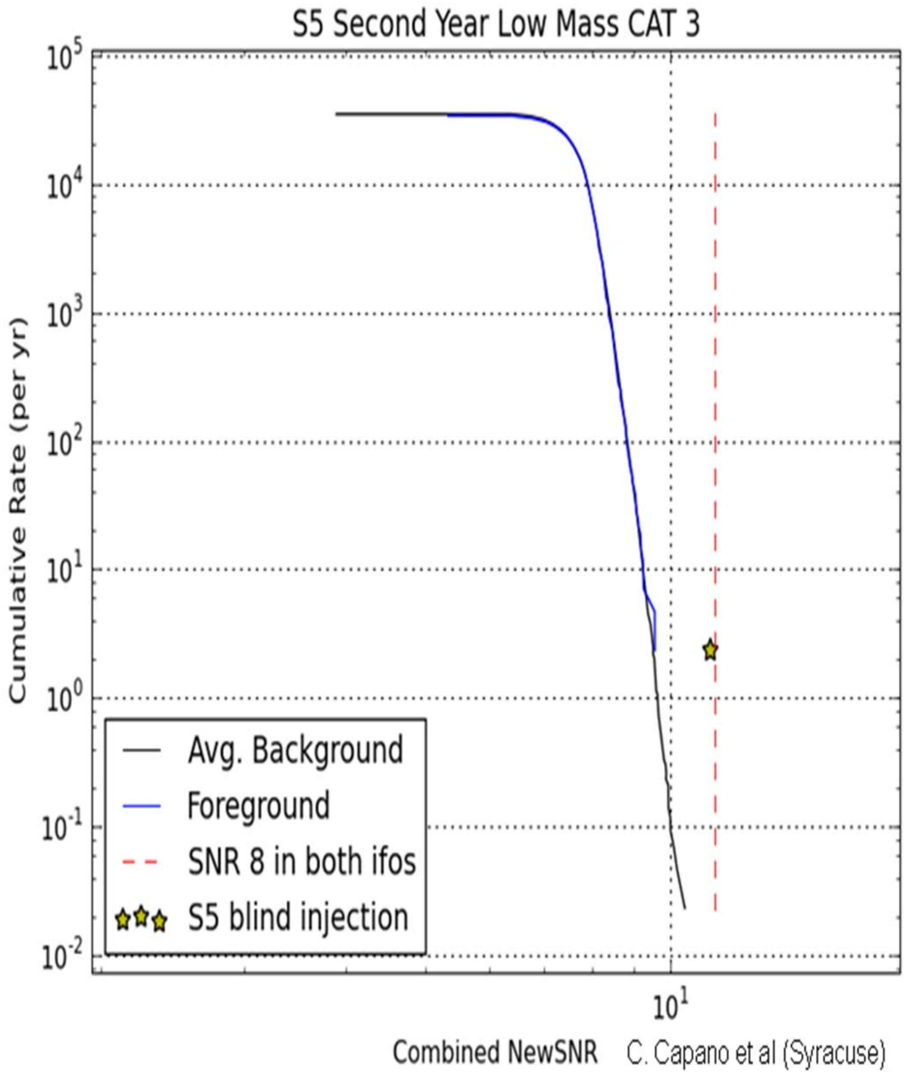

C. Capano et al (Syracuse)

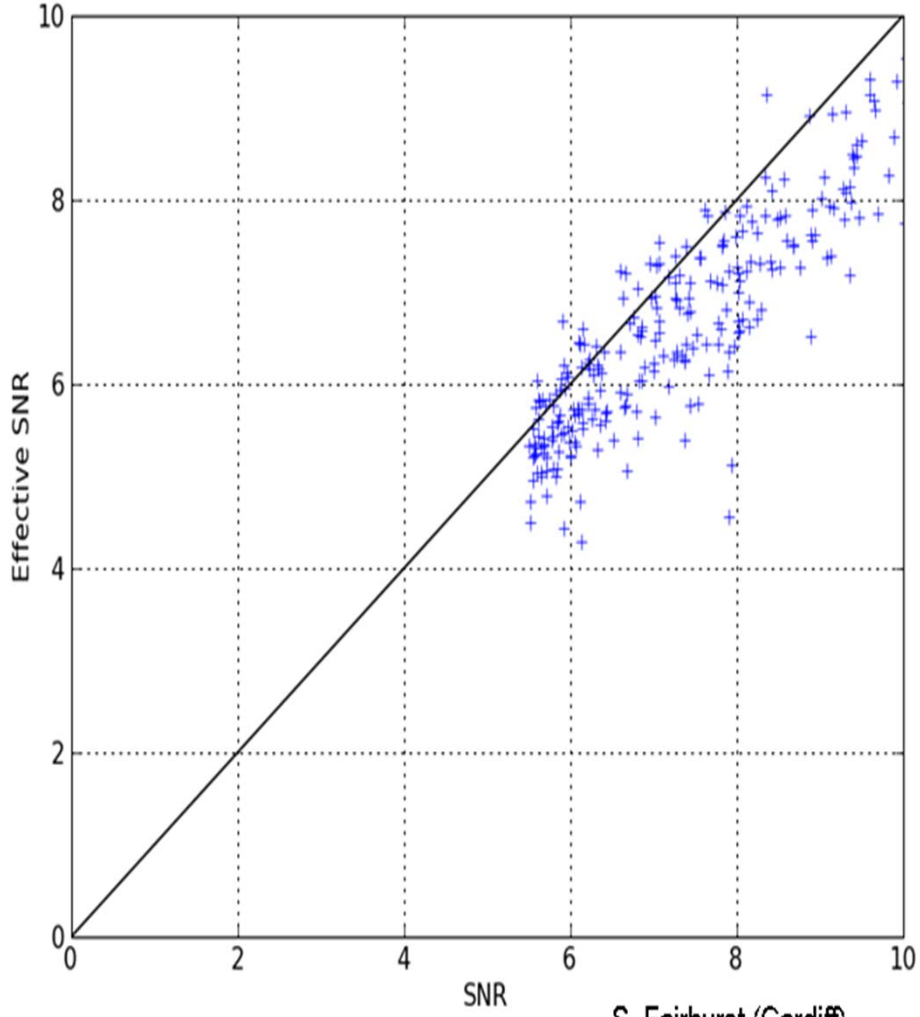

S. Fairhurst (Cardiff)

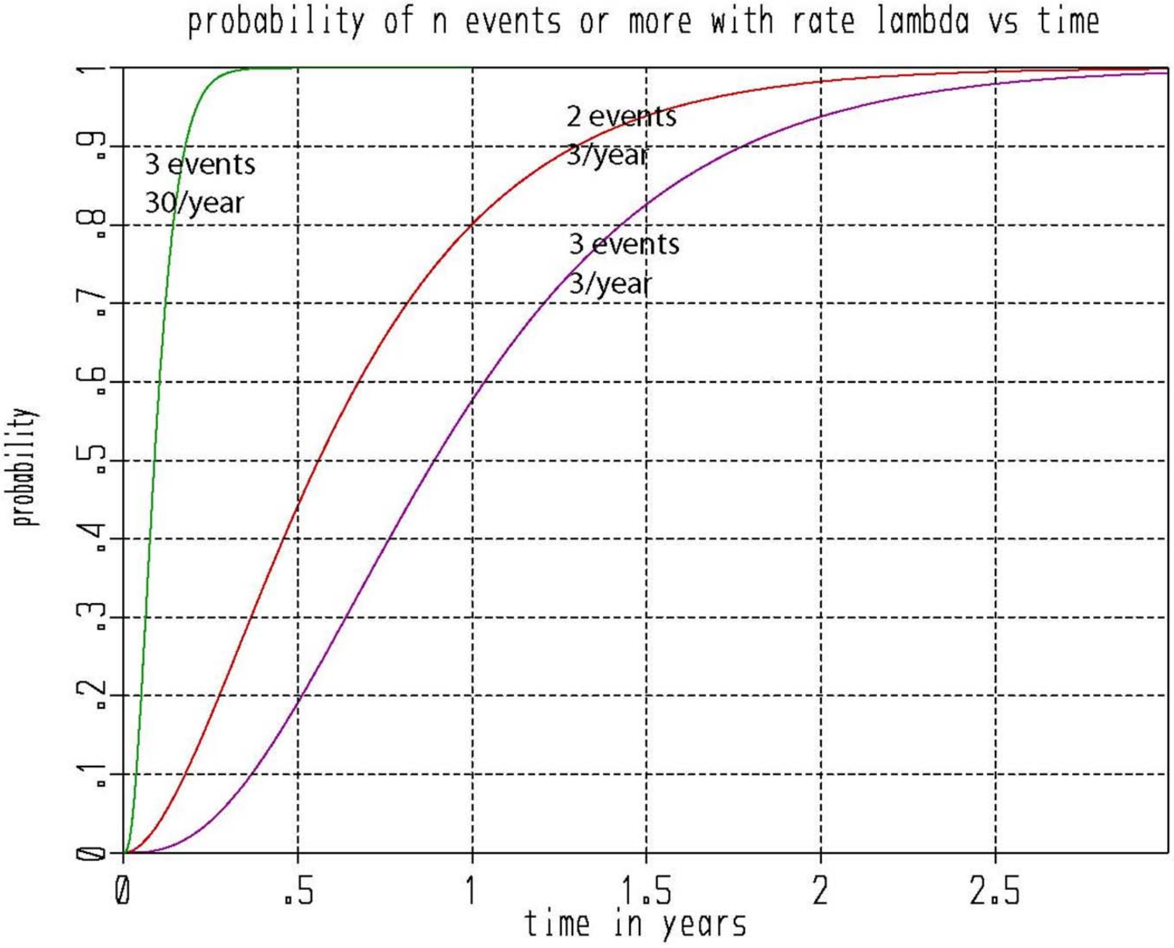
probability of n events or more with rate lambda vs time
probability
0
.1
.2
.3
.4
.5
.6
.7
.8
.9
1
0
.5
1
1.5
2
2.5
time in years
3 events
30/year
2 events
3/year
3 events
3/year

Advanced LIGO H1 Optical Layout

Optical parameters from LIGO-T0900043-08
Coordinates & wedges from T080078-08 & E0900342

December 24, 2009
P. Fritschel
E. Gustafson

D0902838-v2

Arm cavity length	3994.5 m
Power recycling cavity length	57.656 m
Signal recycling cavity length	56.008 m
Input mode cleaner round trip	32.9461 m
Schnupp asymmetry	50.0 mm
Modulation frequencies	f1 = 9.099471 MHz f2 = 45.497355 MHz
Gouy phases (one-way)	PRC: 25 ° SRC: 19 °

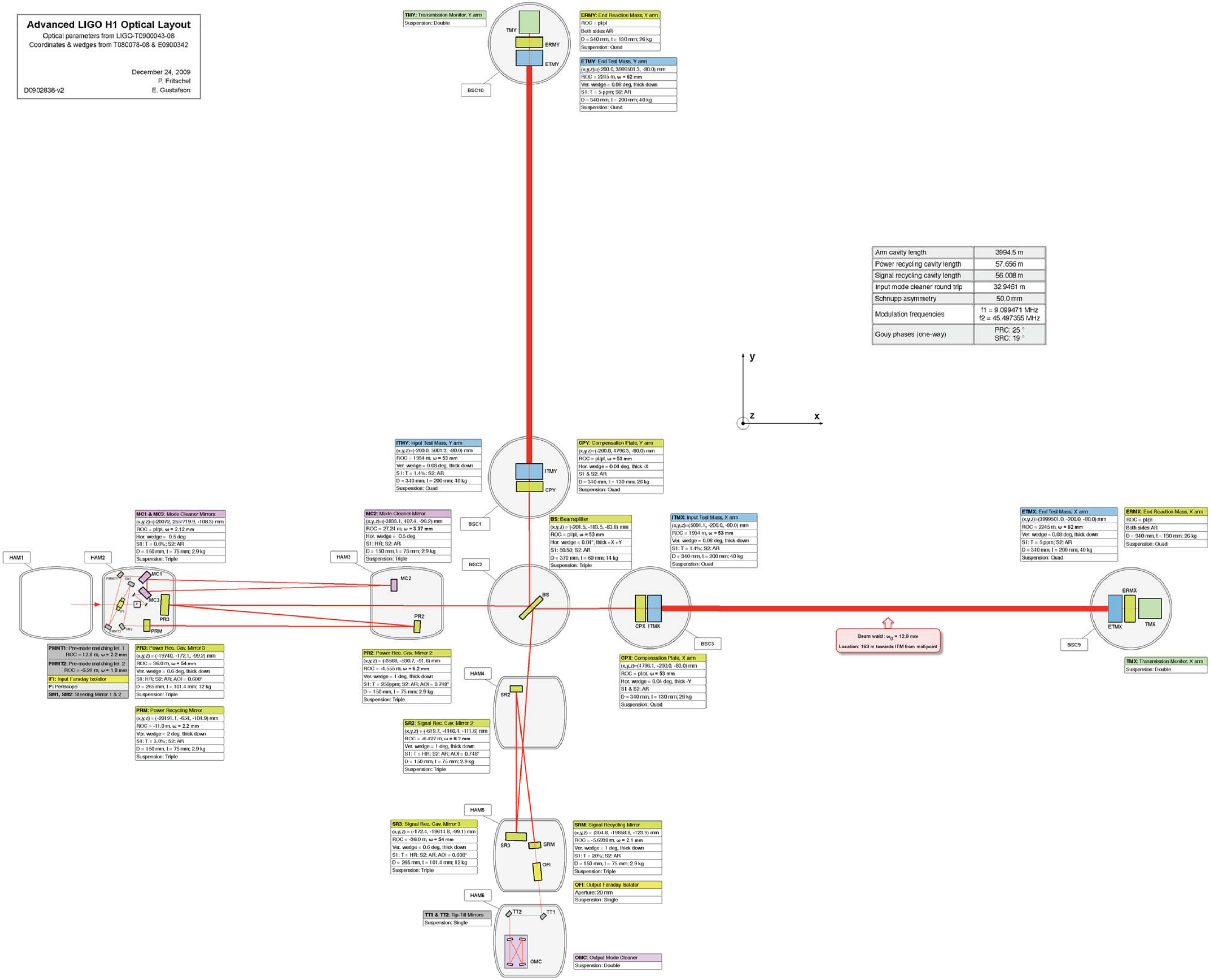

TMY: Transmission Monitor, Y arm
Suspension: Double

ERMY: End Reaction Mass, Y arm
ROC = pl/pl
Both sides AR
D = 340 mm, t = 130 mm; 26 kg
Suspension: Quad

ETMY: End Test Mass, Y arm
(x,y,z)=(-200.0, 3999501.3, -80.0) mm
ROC = 2245 m, **ω = 62 mm**
Ver. wedge = 0.08 deg, thick down
S1: T = 5 ppm; S2: AR
D = 340 mm, t = 200 mm; 40 kg
Suspension: Quad

ITMY: Input Test Mass, Y arm
(x,y,z)=(-200.0, 5001.3, -80.0) mm
ROC = 1934 m, **ω = 53 mm**
Ver. wedge = 0.08 deg, thick down
S1: T = 1.4%; S2: AR
D = 340 mm, t = 200 mm; 40 kg
Suspension: Quad

CPY: Compensation Plate, Y arm
(x,y,z)=(-200.0, 4796.3, -80.0) mm
ROC = pl/pl, **ω = 53 mm**
Hor. wedge = 0.04 deg, thick -X
S1 & S2: AR
D = 340 mm, t = 130 mm; 26 kg
Suspension: Quad

MC1 & MC3: Mode Cleaner Mirrors
(x,y,z)=(-20072, 255/719.9, -108.3) mm
ROC = pl/pl, **ω = 2.12 mm**
Hor. wedge = 0.5 deg
S1: T = 0.6%; S2: AR
D = 150 mm, t = 75 mm; 2.9 kg
Suspension: Triple

MC2: Mode Cleaner Mirror
(x,y,z)=(-3833.1, 487.4, -98.2) mm
ROC = 27.24 m, **ω = 3.37 mm**
Hor. wedge = 0.5 deg
S1: HR; S2: AR
D = 150 mm, t = 75 mm; 2.9 kg
Suspension: Triple

BS: Beamsplitter
(x,y,z) = (-201.5, -183.5, -83.8) mm
ROC = pl/pl, **ω = 53 mm**
Hor. wedge = 0.04°, thick +X +Y
S1: 50/50; S2: AR
D = 370 mm, t = 60 mm; 14 kg
Suspension: Triple

ITMX: Input Test Mass, X arm
(x,y,z)=(5001.1, -200.0, -80.0) mm
ROC = 1934 m, **ω = 53 mm**
Ver. wedge = 0.08 deg, thick down
S1: T = 1.4%; S2: AR
D = 340 mm, t = 200 mm; 40 kg
Suspension: Quad

ETMX: End Test Mass, X arm
(x,y,z)=(3999501.0, -200.0, -80.0) mm
ROC = 2245 m, **ω = 62 mm**
Ver. wedge = 0.08 deg, thick down
S1: T = 5 ppm; S2: AR
D = 340 mm, t = 200 mm; 40 kg
Suspension: Quad

ERMX: End Reaction Mass, X arm
ROC = pl/pl
Both sides AR
D = 340 mm, t = 130 mm; 26 kg
Suspension: Quad

Beam waist: ω_0 = 12.0 mm
Location: 163 m towards ITM from mid-point

TMX: Transmission Monitor, X arm
Suspension: Double

PMMT1: Pre-mode matching tel. 1
ROC = 12.8 m, **ω = 2.2 mm**
PMMT2: Pre-mode matching tel. 2
ROC = -6.24 m, **ω = 1.8 mm**
IFI: Input Faraday Isolator
P: Periscope
SM1, SM2: Steering Mirror 1 & 2

PR3: Power Rec. Cav. Mirror 3
(x,y,z) = (-19740, -172.1, -99.2) mm
ROC = 36.0 m, **ω = 54 mm**
Ver. wedge = 0.6 deg, thick down
S1: HR; S2: AR; AOI = 0.608°
D = 265 mm, t = 101.4 mm; 12 kg
Suspension: Triple

PRM: Power Recycling Mirror
(x,y,z) = (-20191.1, -654, -104.9) mm
ROC = -11.0 m, **ω = 2.2 mm**
Ver. wedge = 2 deg, thick down
S1: T = 3.0%; S2: AR
D = 150 mm, t = 75 mm; 2.9 kg
Suspension: Triple

PR2: Power Rec. Cav. Mirror 2
(x,y,z) = (-3588, -530.7, -91.8) mm
ROC = -4.555 m, **ω = 6.2 mm**
Ver. wedge = 1 deg, thick down
S1: T = 250ppm; S2: AR; AOI = 0.748°
D = 150 mm, t = 75 mm; 2.9 kg
Suspension: Triple

CPX: Compensation Plate, X arm
(x,y,z)=(4796.1, -200.0, -80.0) mm
ROC = pl/pl, **ω = 53 mm**
Hor. wedge = 0.04 deg, thick -Y
S1 & S2: AR
D = 340 mm, t = 130 mm; 26 kg
Suspension: Quad

SR2: Signal Rec. Cav. Mirror 2
(x,y,z) = (-619.7, -4160.4, -111.6) mm
ROC = -6.427 m, **ω = 8.2 mm**
Ver. wedge = 1 deg, thick down
S1: T = HR; S2: AR; AOI = 0.748°
D = 150 mm, t = 75 mm; 2.9 kg
Suspension: Triple

SR3: Signal Rec. Cav. Mirror 3
(x,y,z) = (-172.4, -19614.8, -99.1) mm
ROC = -36.0 m, **ω = 54 mm**
Ver. wedge = 0.6 deg, thick down
S1: T = HR; S2: AR; AOI = 0.608°
D = 265 mm, t = 101.4 mm; 12 kg
Suspension: Triple

SRM: Signal Recycling Mirror
(x,y,z) = (304.8, -19858.8, -123.9) mm
ROC = -5.6938 m, **ω = 2.1 mm**
Ver. wedge = 1 deg, thick down
S1: T = 20%; S2: AR
D = 150 mm, t = 75 mm; 2.9 kg
Suspension: Triple

OFI: Output Faraday Isolator
Aperture: 20 mm
Suspension: Single

TT1 & TT2: Tip-Tilt Mirrors
Suspension: Single

OMC: Output Mode Cleaner
Suspension: Double

NS/NS binary inspiral triggers in the year 1 of S5 in L1 and H1

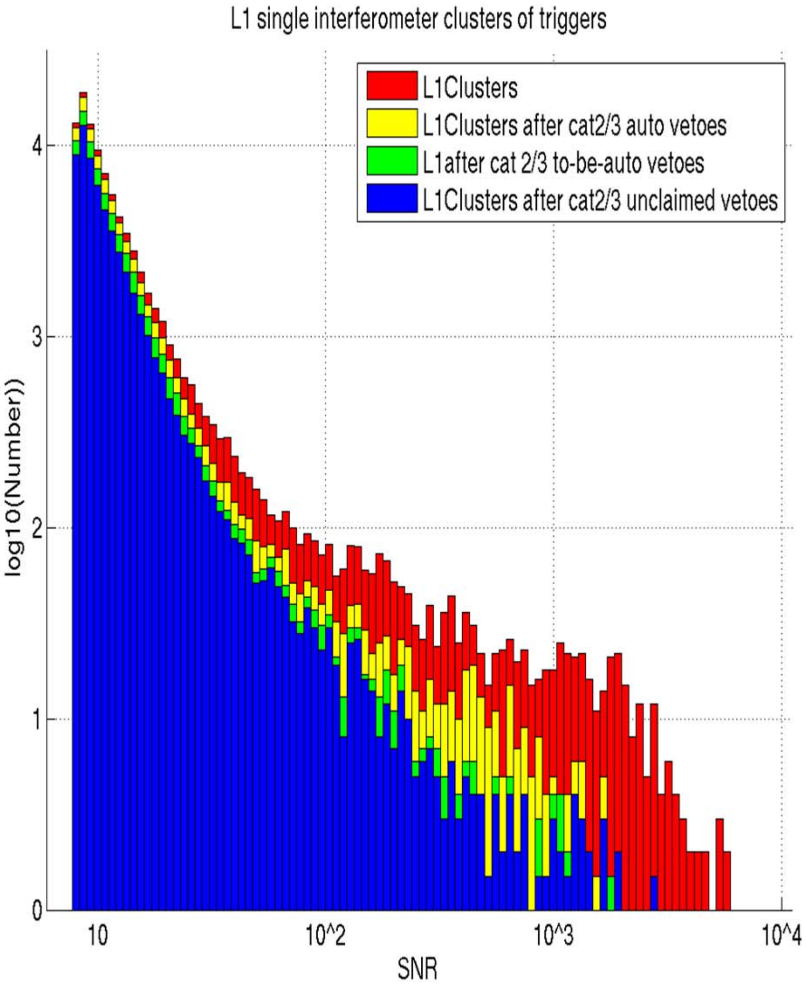

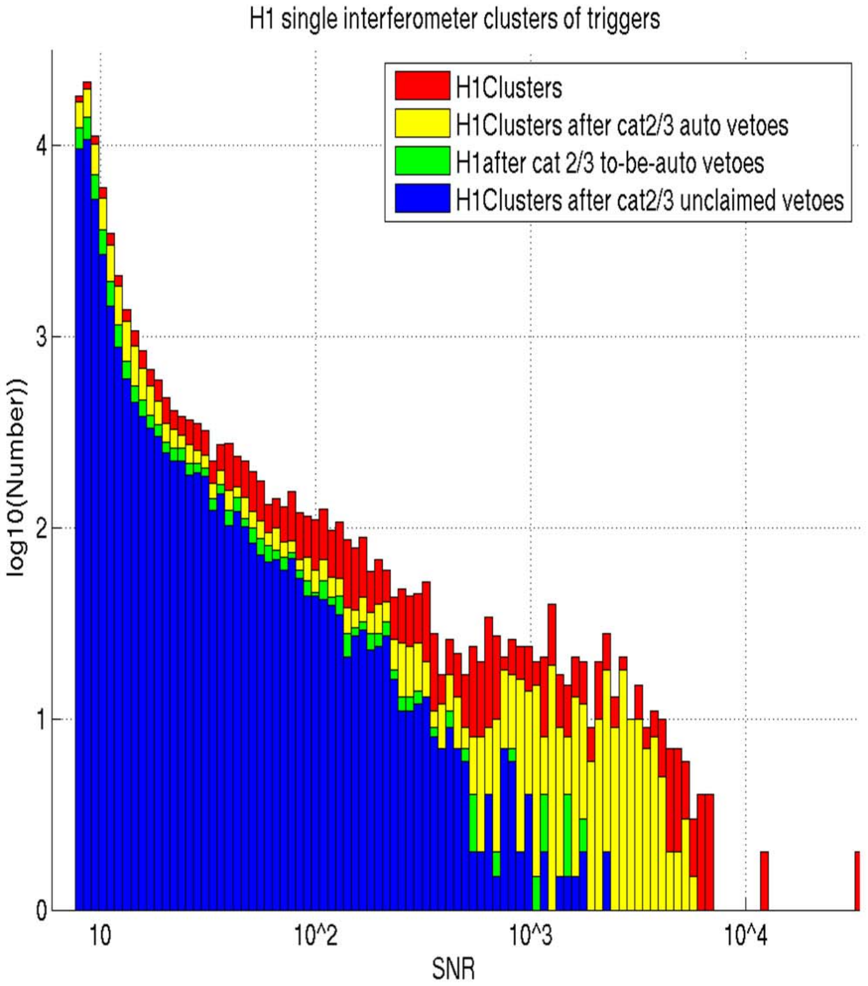

Jake Slutsky   LSU

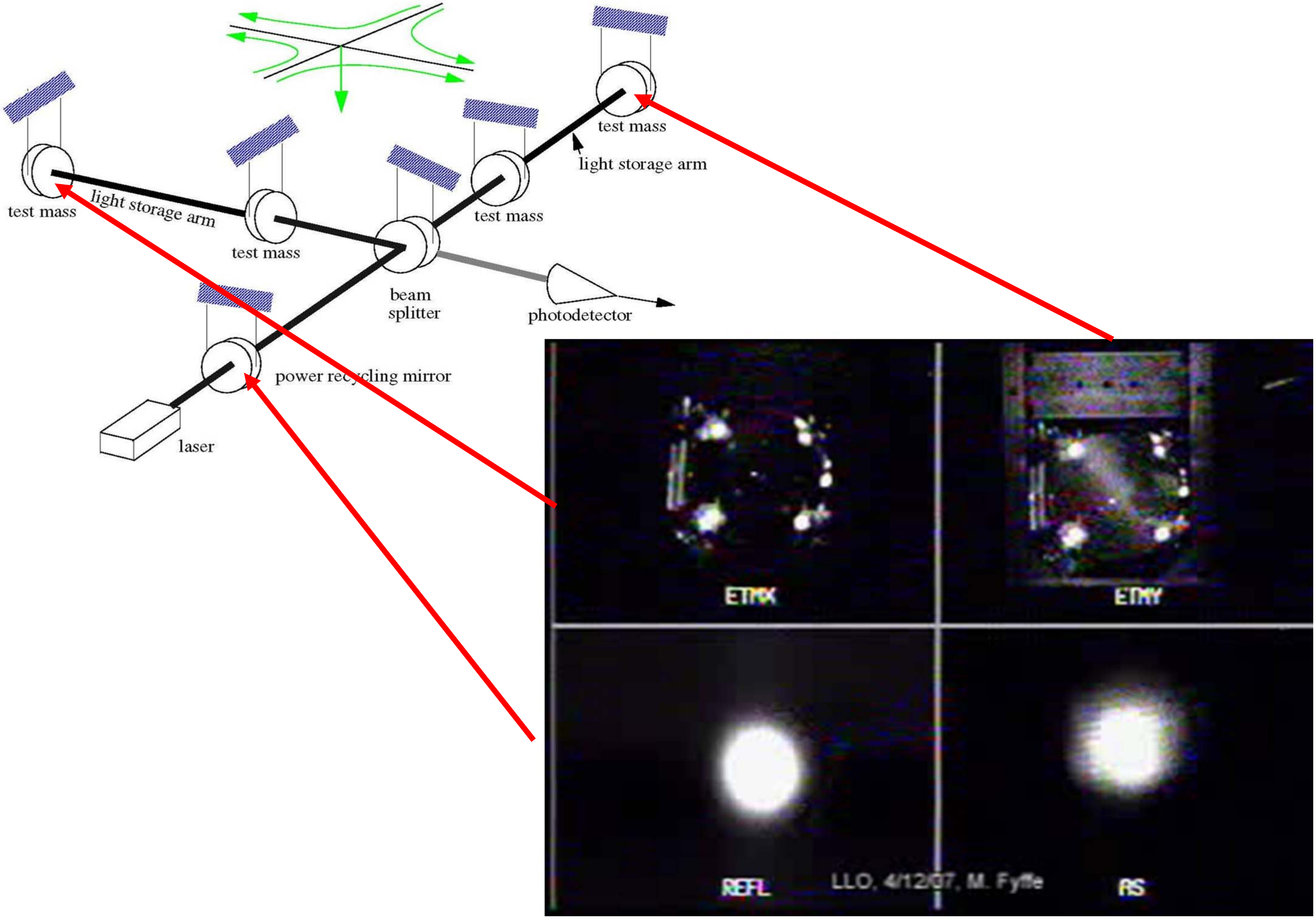
test mass
light storage arm
test mass
test mass
beam
splitter
test mass
light storage arm
test mass
photodetector
power recycling mirror
laser
ETMX
ETMY
REFL
LLO, 4/12/07, M. Fyffe
AS